The United Graduate School of Agriculture Sciences, Iwate University (UGAS)

Yamagata University, Faculty of Agriculture

Doctoral Thesis

# Understanding forest ecosystems in steep mountains using Unmanned Aerial Vehicles, Yamagata, Japan

GONROUDOBOU OROU BERME HERVE

Yamagata, Japan 2022

**Table of Contents**

**Table of Figures**

**List of Acronyms**

| | |
|---|---|
| CHM | Canopy Height Model |
| DSM | Digital Surface Model |
| GNSS | Global Navigation Satellite System |
| GPS | Global Positioning System |
| nDSM | Normalized Digital Surface Model |
| RGB | Red – Green – Blue |
| ROI | Region of Interest |
| SfM | Structure from Motion |
| TAF | Terrain awareness function |
| NTAF | Non terrain awareness function |
| UAV | Unmanned Aerial Vehicle |

**Acknowledgement**

More than an academic step my PhD years has been a whole experience. To achieve this milestone today, it is not only my effort but also the efforts, from everyone around who supported me during my research.

I would like to express my gratitude to Professor Larry Lopez for first giving me the opportunity to join his team and for the full support.

Special thanks to Professor Yago Diez for his kind support and helping to develop algorithm, discussing and orienting.

I am grateful to my co-supervisors for they time and they helpful comment

Thanks to all the lab member for helping.

Thanks to Ms. Mizuki Hasegawa for kindly and patiently supporting

Many thanks to my parents GONROUDOBOU Orou Deke and SOULEY Afoussatou. My special gratitude also goes to my sister who create the contact with Professor Larry.

**Summary in English**

In Japan, forests cover 68% of the whole territory and they distribute extensively in steep mountains. Mountain forests provide valuable support to watershed bio-activities, ecosystems with complex structure and composition . Most of watersheds are composed of natural forests and of forest. These forest ecosystems are of difficult accessibility and many of their characteristic such as growth healthy composition are unknown.

In recent years, Unmanned Aerial Vehicle (UAV) have become available for civilian use and in a short period of time has become one of the most essential tools in the study of natural ecosystems and especially on the investigation of forests where terrain constraints the access to close observations or measurements. UAV provide very high resolution of spatial and temporal data with high flexibility of maneuvering. Modeling of forests using overlapped UAV-acquired images and the photogrammetry technique, known as structure from motion (SfM) makes it possible to obtain highly detailed 3D information of forest ecosystems. Thus, UAV is a reliable alternative to the traditional energy time consuming field work or to the imprecise (because of poor resolution) satellite images. Different sensors can be attached to UAVs but Digital RGB cameras have shown to be cost efficient and the most versatile sensor to capture forest characteristics with a high level of detail.

Numerous methodologies and approaches are used to take full advantage of UAV images information, but the topography, specifically steep terrain, is an important factor to be taken into consideration for the interpretation of those images. Thus, the image quality or the correct representation of forests in steep slopes improves the overall understanding of the forest ecosystems, since the position of trees along the slope are considered in the image analysis. Terrain relief variability compromises the ground sampling distance (GSD) homogeneity and the image details along the slopes (mainly in the lower section of the slopes) since the flying

height of UAVs is always higher than that at the top of the slope, when the UAV is flying at a fixed height.

Therefore, in the first chapter of this study, UAV-acquired images were collected taken into account the terrain and the performance of algorithms on the generated images after processing was conducted. The terrain awareness function (TAF) provided by the DroneDeploy software is based on publicly available digital surface model (DSM) with a coarse resolution which allows the UAV (Mavic 2 Pro) to follow the relief of the terrain. Thus, the UAV always keeps the flying height in relation to the ground, regardless of the position along the slope. The performance of TAF in the flying mission is compared with a flying mission where TAF was not used (NTAF) and the UAV is flown at a constant height, meaning that the forest at the upper part of the slope is closer to the UAV and the forest at the bottom of the slope is further from it.

The study area was dominated by fir (*Abies mariesi*) trees on a 20-degree slope. In order to test the improvement of image quality on the orthomosaics and the Canopy Height Model (CHM) an encode tree elevation value file produced by using TAF and NTAF, two algorithms were used to automatically find trees (treetop detection) in the forest. On the one hand, Algorithm 1, connected component, was a sliding window-based approach that screen the CHM altitudes of the pixels in decreasing order building trees canopy and then assigning a point to the maxima. On the other hand, Algorithm 2 point at the maxima height after applying several morphological operations. When using TAF, the dense point clouds (DPCs) were denser and more homogeneously distributed along the slope than when using NTAF. Algorithm 1 showed a 5% improvement in treetop detection accuracy when using TAF (86.55%), in comparison to NTAF (81.55%), at the minimum matching error of 1 m. In contrast, when using algorithm 2, treetop detection accuracy reached 76.23% when using TAF and 62.06% when

using NTAF. Thus, for only treetop detection, NTAF can be sufficient when a sensitive algorithm such as Algorithm 1 is used. However, TAF showed more precision by less tree matched more than one to the ground truth point (3.2%) of detected treetops at 2m margin error. Repeated points, led to an overestimation of detected treetops.

In the second chapter we assessed TAF treetop detection improvement threshold in a steeper slope (28°) and complex terrain using algorithm 2. The hypothesis was that in a steeper slope a higher difference in the treetop detection algorithm would be found. The study site was a mature cedar forest. TAF was based on self-generated DSM (not publicly available as in the previous case), which is expected to improve the quality of flying path of the UAV. We assess the performance of treetop detection algorithm in comparison to NTAF during UAV data acquisition data. Our study site was a mountainous complex terrain. Most of the treetops were detected. The result shows 93.95% of treetops detected when using TAF and 91.42% when using NTAF with a 2.5m margin of error. Using TAF decreased matching repetition and even in highly sharp slope terrain the improvement was smaller than expected.

In the chapter 3, TAF (to assure homogenous orthomosaic quality) and a semi-automatic python tree species classifier was used for four tree species mapping in a mixed forests composed of beech (*Fagus crenata*), oak (*Quecus crispula*), larch (*Larix kaempferi*) and maple (*Acer spp.*). In this forest, the analysis of Nitrogen stable isotope ($\delta^{15}N$) and N concentration from foliar samples was performed. The results of individual trees were extrapolated from tree to mixed forest stand Nitrogen distribution using the automatic tree species classification and their model distribution within the forest. Thus, using high quality UAV acquired image orthomosaic in steep terrains, automatically detected tree distribution and biophysiological parameters were combined.

**Summary in Japanese**

世界の陸地の 25%を山地が占めている。日本では国土の 68%が森林に覆われており。それは急傾斜の山々に広く分布している。山林は流域の生物の活動を支える重要な役割を担っているが、その生態系の構造や構成はまだよく解明されていない。流域のほとんどは天然林で構成されているが、人工林や高地にある森林ではよりモノカルチャーとなっている。

近年、無人航空機(UAV)が民間でも利用できるようになり、短期間のうちに自然生態系の研究、特に接近しての観察や測定が制限される地形の森林調査において必要不可欠なツールのひとつとなりつつある。UAV は空間的、時間的に非常に解像度の高く、柔軟性の高いデータを我々に提供してくれる。3 次元構造復元(SfM)として知られている UAV で得られた画像を重ね合わせて森林をモデル化する写真測量技術によって、森林生態系の高度で詳細な 3D 情報を取得することが可能である。したがって、UAV は従来のたくさんのエネルギーと長い時間を消費するフィールドワークや低解像度のために精密でない衛星画像に変わる信頼性の高い手法である。UAV には様々なセンサーを取り付けることができるが、森林の特徴を詳細に捉えるために、デジタル RGB カメラは費用効率が高く、最も万能な手段である。

UAV の画像情報を最大限に活用するために非常に多くの方法論とアプローチが用いられているが、それらの画像の解像を考慮することが地形、特に急斜面の地形においては大切である。よって、画像分析では斜面にある木々の位置が考慮されるため、画像の質や急斜面な森林を正しくモデル化することは森林生態系の全体的な理解を高める。UAV が一定の高さで飛ぶ場合、その高さは常に傾斜の最高高度よりも高いため、地形の起伏の変化によって、地上解像度(GSD)の均一性や主に底部における斜面の画像の詳細が損なわれることがある。

そこで、本研究の第一部では、地形を考慮して UAV からの画像を取得し、処理後の画像から生み出されたアルゴリズム性能を分析した。DroneDeploy ソフトウェアによって提供されている地形認識機能(TAF)は一般に利用可能な解像度の粗いデジタル地表モデル(DSM)基づいており、UAV (Mavic 2 Pro)は地形の起伏に沿って飛ぶことができる。よって、斜面に沿う位置に関わらずに、UAV は常に地表との距離に基づ

いた高さを飛行する。TAF を用いた飛行任務の性能は、UAV が TAF を用いずに飛行した飛行任務(NTAF)と比較された。NTAF では UAV が常に一定の高さで飛ばされ、それは斜面の上部では UAV が地形の近くを飛行し、底部では地形からさらに離れた空中を飛行することになる。

調査地はトドマツ(*Abies mariesii*)が優占種となっている傾斜 20 度の斜面である。オートモザイク画像と TAF、NTAF によって作られた林冠高さモデル(CHM)の質を高めるために、森林の木々(梢の検出)が自動的に検知できるように 2 つのアルゴリズムが用いられた。コネクテッドコンポーネンツであるアルゴリズム 1 はスライディングウィンドウの手法で、ピクセルの CHM 高度を降順に並べて林冠を構成する木々を検出したうえで、最大値にポイントを割り当てる。他方、アルゴリズム 2 はいくつかのモルフォロジー演算を適用した後に最大値を割り当てた。その結果、TAF で飛行した場合、NTAF で飛行した場合よりも高密度ポイントクラウド(DPCs)が地形に沿ってより高い密度で、より均一的に分散されていた。アルゴリズム 1 においては、最小マッチング誤差が 1m で、NTAF で飛行した場合の正確度が 81.55%であったのに対し TAF で飛行した場合の正確度は 86.55％と、梢(樹木の最上部)の検出精度が 5%高まった。それに対しアルゴリズム 2 を使用した場合は、梢の検出精度は TAF で飛行した場合で 76.23%、NTAF で飛行した場合で 62.06%であった。よって、梢の検出に限っては、NTAF はアルゴリズム 1 のような緻密なアルゴリズムを用いた場合において有効であると言える。しかしながら、TAF では 2m の誤差で梢の検出をする割合がわずか(3.21%)であり、より高精度であることが示された。折り返し地点では梢が過大に検出される。

第二部では、アルゴリズム 2 を用いた際に、より急傾斜(傾斜 28 度)で複雑な地形構造において TAF は梢の検出の基準値を向上することを評価した。仮説は、より急斜面では梢の検出アルゴリズムに、より高い差異が見られるだろうというものであった。調査地は十分に成長しきったスギ林である。TAF は自動で生成される DSM(ただし、前回のように一般に利用可能ではない。)に基づいていており、それは UAV の飛行コースの質を高めると期待される。我々は UAV データの取得データに、NAFT と比較して梢検出アルゴリズムの性能を評価する。我々の調査地は起伏の複雑な山々である。大半の梢は検出された。その結果、2.5ｍを最大許容誤差と設定した時、

TAF では 93.95%で、NTAF では 91.42%で梢が検出された。TAF を使うとマッチング頻度が減少し、急勾配の傾斜でさえも予想より向上は小さかった。

最後の部分では、ブナ(*Fagus crenata*)、ミズナラ (*Quecus crispula*)、カラマツ(*Larix kaempferi*) 、カエデ(*Acer monomaxim*)から成る混合林の樹種のマッピングのために TAF(オートモザイク画像の質は均一とする)と Python の半自動樹種判別を用いた。この森林では、葉のサンプルから窒素安定同位体($^{15}N$)と窒素の濃度が分析され、各個体の木々から得られた値は自動樹種判別とその森林内の分布モデルを用いながら混合林全体の値であると推定された。このようにして、急斜面において UAV で得た質の高い空撮画像で作成されたオートモザイク画像を用いることで、自動的に樹木の分布と生物生理学的指標を同時に行った。

# Chapter 1: Background

## 1.1 Background

Mountains forests are found in all over world regions from the north to south hemisphere (Grêt-Regamey and Weibel, 2020). Mountains cover 25% of the world's land surfaceMountain produce heterogeneous environments with high microclimate diversity (Kulonen *et al.*, 2018) lead by temperature, altitude, slope and aspect. Nutrient movement and accumulation across topographic gradient (Tian *et al.*, 2020) creates a variety of plant microhabitat. Mountain watersheds contribute to at least up to 20% of total discharge of fresh water in humid area and more than 50% in arid areas (Messerli, Viviroli and Weingartner, 2004). Mountain forests, about 20 % of world forest can be defined as forests at an altitude above sea level equal or higher than 2500m regardless of the slope, or between 300–2 500 m and a slope with sharp changes in elevation within a short distance (FAO, 2022). Forests in watersheds are the most exposed ecosystem to natural disaster and requires continuous management (Vacik and Lexer, 2014). Climate change significantly increased disturbance occurrences which is challenging for the balance of composition, structure and growth (Hartl-Meier *et al.*, 2014) rate of forest ecosystems. Timber production, tourism, carbon sink are some issues in a wide list of ecological and socio-economic services provided by forests. Mountain forests remain poorly understood ecosystems and even more the effects of global warming on trent. Thus, their sound is one of the most interesting ecosystems to investigate for better understanding, global warming effect assessment and sustainable management. Contemporary forest management challenge includes high demand of data for science community.

Existing forest investigation method are time consuming and manpower demanding. Unmanned Aerial Vehicles (UAV), commonly known as drones and part of Unmanned Aerial System (UAS) have the advantage of providing high quality of temporal and spatial data over a large coverage target area. Drone image high resolutions (up to centimeters level) allow entire

forest view and the capture of individual trees details. Overlapped UAV acquired images advance modeling using photogrammetry structure from motion (SfM) produces high-value spatial information in the form of dense point clouds, textured polygonal models, georeferenced true orthomosaics and DSMs/DTMs for post-processing and analysis tasks. UAVs can collect images over 100 hectare (ha) a day of complex terrain with good flexibility. UAV is now an essential tool for monitoring of forest ecosystems. Various sensors can be mounted on UAVs platform and performs differently base on data needed; multispectral sensors provide deep individual trees condition (Kopačková-Strnadová *et al.*, 2021) and their response is related to the close environmental conditions while laser sensor perform better for 3D mapping (Li *et al.*, 2019). Digital RGB Cameras are the most cost effective and general task payload providing good precision data set for direct data interpretation. With these images it is possible to rapidly and accurately accomplish tasks such as spatial mapping and dendrometric parameters measurement (Chakraborty *et al.*, 2019), biomass calculation (Jayathunga, Owari and Tsuyuki, 2019), health conditions monitoring based on the visualizations of canopies (Nguyen *et al.*, 2021; Leidemer *et al.*, 2022), individual tree detection and species classification (Ferreira *et al.*, 2020). Emerging technologies such as computer vision and deep learning combine with classic visual image treatment showed to be useful for deep spectral analysis and lead progressively to automatic data management (Cabezas *et al.*, 2020; Ferreira *et al.*, 2020; Kentsch *et al.*, 2020). Even do UAVs have shown to be a powerful tool for describing special characteristics in science application, this field is on building and can opposed limitation on providing some kind of information such as tree physiological process. As attempted numerous time, scaling up from tree to forest stand by combining field survey and remote sensing image, forest inventory base or vegetation map (Čermák, Kučera and Nadezhdina, 2004; Lecointe *et al.*, 2006) is relevant for forest stand level monitoring.

Numerous methodologies are used to extract efficiently the must information possible from images and thus, improving those image quality from the beginning are expected to make a net improvement on analysis performance. Reconstruction into higher resolution using random forests learning methods (Schulter, Leistner and Bischof, 2015) or terrain variation data integration into UAV automatic flight mission can significantly improve data quality along slopes. Small features are hardly detectable with low resolution images usually at the lower section of the slopes when flying at constant altitude (Battulwar et al., 2020) . Most studies using UAVs considering terrain awareness flights have focused on geomorphic change detection such as volcanos, landslides, glaciers, a gorge, or mine pit in different parts of the world (Niethammer et al., 2012; Cook, 2017; Rossini et al., 2018; Valkaniotis, Papathanassiou and Ganas, 2018; Battulwar et al., 2020). However, there is almost no study focused on the effect of slope on image quality or the effect on the DPC, which is essential information for reconstructing 3D characteristic of forests.

### 1.1.1 Objective

The aim of this thesis is to improve. UAV acquired images collection optimization methods in steep terrain and computer vision technique application in post processing analysis.

Through this thesis I focused on terrain variation effect on drone image resolution along steep slopes and approaches to homogenized image quality over the covered areas. In -this study, I integrated digital surface model (DSM) in UAV automatic path planning and access how improved is computer vision algorithm performance in canopy height model (CHM) base treetop detection. I intended to provide useful, practical and easy applicable information about the efficient use of UAV for forest experts and managers. The study also attempts to provide techniques to scale up from fieldwork measurements to stand level using remote sensing image.in this study in particular we focus on nitrogen content and isotope values results from

tree to forest stand level. This is an additional way to take full advantage of UAV technologies and valorized field work and existing data.

In order to accomplish the major objectives of this study are presented below:

1. To evaluate the performance of a treetop detection algorithms on the CHMs obtained when using Terrain Awareness Function and when it is not used.
2. To evaluate slope steepness and DSM resolution effect on TAF CHM base treetops detection algorithm.
3. Scaling up from plot to forest level using field work and drone acquired image analysis in complex terrain and coverage forest.

### 1.1.2 Structure of the Study

The study is divided into five sections (figure 1).

I. UAV image collection, in this section I set the flight mission including different resolution of elevation grid.

II. Images preprocessing: photogrammetric and SfM processing of digital images and generation of 3D spatial dense point cloud (DPC), DSM and orthomosaic.

III. Canopy height model (CHM) generation and data preparation

IV. Treetops detection algorithms application and data validation: here was computer vision technique application into CHM when flying at constant height and using terrain awareness function. The regions of interest were on slightly sharp slop (chapter 2) and more dramatic slop (chapiter 3) including real resolution terrain awareness.

V. Nitrogen scaling up from plot to forest stand: chapiter 4 dedicated to this section was an application of the results from chapter 2 and 3. Here I attempted a scaling up of

field work plot nitrogen value at forest stand level based on the structure and composition of mixed forest obtained from UAV orthomosaic

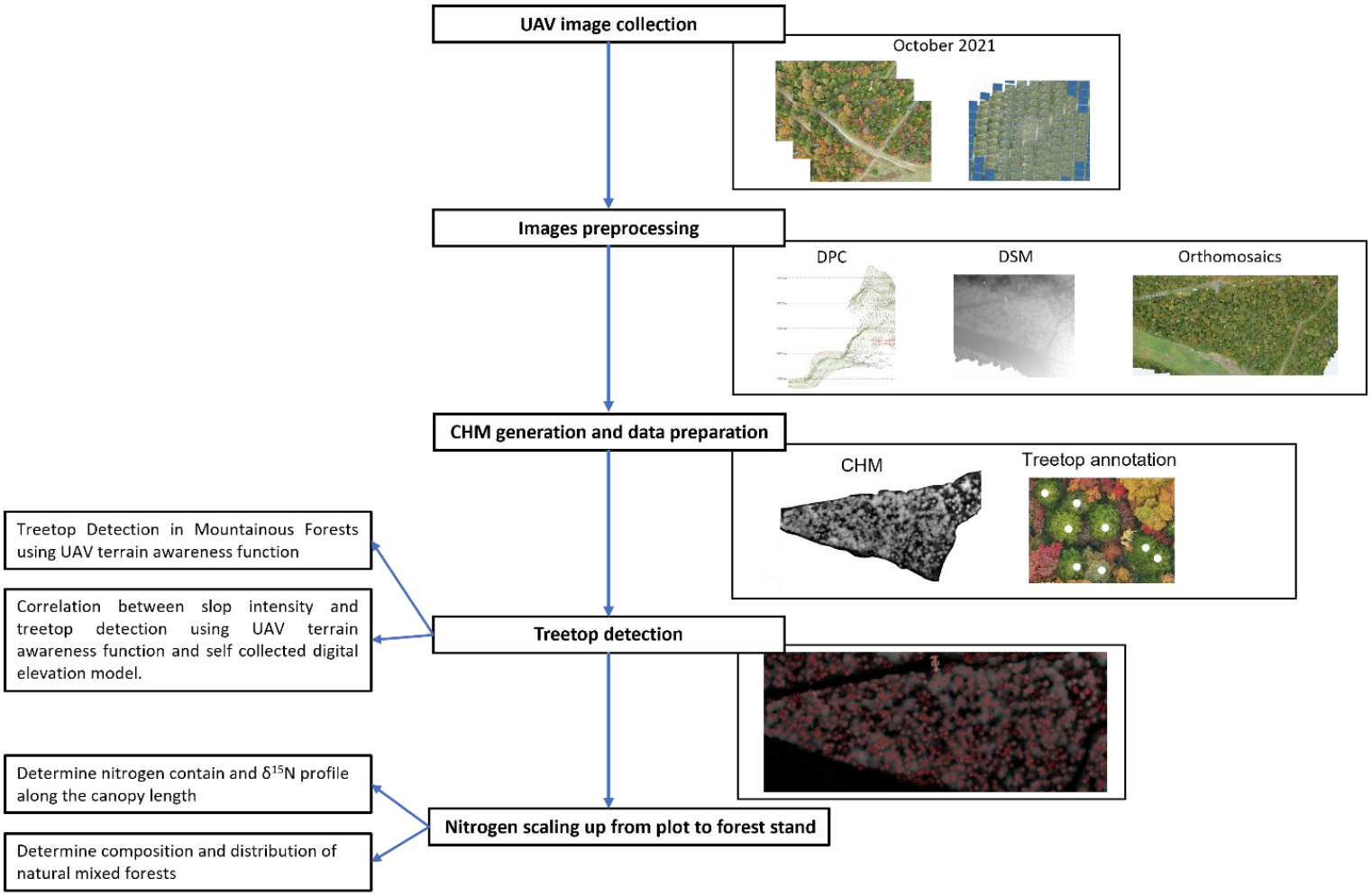


**Figure 1.1:**Structure of the study.

## 1.2 Scope

Forest in steep slope is found all over the world. Terrain variation leads to an heterogenous image resolution along the slope that can make user miss valuable details on the covered area. Even do sensitive photogrammetry software can handle objects proportion variability, some distortions are still perceptible. Several studies have address terrain morphologies into UAV flight mission but there were almost all oriented to the terrain itself than the coverage. Good

image quality is a key requirement for UAV image analysis. In this study I proposed to fly UAV missions using terrain awareness function with different source of DSM on different sharpness degree terrain. The results will provide good information for scientist and forest professional about optimal use of UAV in steep slope but also how to make use of high-resolution UAV image to scale up field survey result to forest stand level.

# Chapter 2: Treetop Detection in Mountainous Forests using UAV terrain awareness function

## 2.1 Introduction

Forests in steep terrains are found all over the world and in fact are more abundant than those in flat areas, where they have already been cut for human settlements or agriculture activities. One of these cases is Japan, where most of the 68% forest coverage, is found in steep mountains slopes ranging from 35 to 45 degrees (Forestry Agency, Japan, 2019). Forest surveys under these conditions limit the access to a small set of sample plots, where ground measurements can be conducted, constraining the understanding of the larger rest. Until recent years, satellite images were widely used tools to capture large forest areas with a reasonable level of detail, depending on the resolution of the images and most importantly their cost. In these images the uneven terrain of mountains is taken for granted and the problem of resolution and errors caused by the slope are accepted. Over the years studies have dealt with the design of following terrain applications for aircrafts and it is just until recently that this function has become an important issue for flight plans of UAVs (Unmanned Aerial Vehicles) over steep terrains. Most studies using UAVs considering following terrain flights have focused on geomorphic change detection such as volcanos, landslides, glaciers, or a gorge in different parts of the world (Niethammer *et al.*, 2012; Cook, 2017; Rossini *et al.*, 2018; Valkaniotis, Papathanassiou and Ganas, 2018; Manconi *et al.*, 2019), but to our knowledge none has focus on forest characteristics in steep terrains. Some of the authors in these studies have described a clear strategy to deal with the issue of following the terrain. (Manconi *et al.*, 2019) tackled the problem of slopes by flying automatically and manually in stripes at different altitudes.

The result of flying at different altitudes in separate flight plans or flying manually to keep the same altitude of the UAV to the ground along slopes, is that in the first case blank spots are produced in the orthomosaic and in the second case keeping the overlapping of successive images is compromised. This is especially relevant when the focus is the detail information of dendrometric parameters of forests, since tree characteristics appear different depending on the

position within the slope. Recent UAV applications on forestry research have shown the immense potential of the very high-resolution images for capturing individual tree details (Safonova *et al.*, 2019; Kentsch *et al.*, 2020; Nguyen *et al.*, 2021), however the issue of following the terrain has not been addressed, even though the differences might have a significant effect on the perception of the tree canopy area, density of the points cloud and the canopy height model at different positions along the slope. No information concerning following the terrain is found neither in the thorough reviews of UAVs in forestry (Torresan *et al.*, 2017) nor the review of application of Deep Learning on forestry using UAVs imagery (Diez *et al.*, 2021). The extraction of more detailed information is important for the precise estimation of forest dendrometric parameters (Puliti *et al.*, 2015), forest health (Näsi *et al.*, 2015), gaps and forest species composition (Getzin, Nuske and Wiegand, 2014).

Thus, UAVs flight plans that include the terrain awareness function (TAF) will keep the same Ground Sampling Distance (GSD) and capture the characteristics of not only the treetop of dominant trees but also those in the co-dominant and even suppressed layer within the forest structure. (Kozmus Trajkovski, Grigillo and Petrovič, 2020) showed that the precision using TAF is enhanced when users create their own Digital Surface Model (DSM) of a given slope to guide the UAV, as these data are input in the flight plan of the UAV, when following the terrain. However, this cannot be done in most of low-cost commercial UAVs such as the Mavic 2 Pro for which applications such as drone deploy, provide the following awareness function using the available world digital terrain data (SRTM, etc.)

Individual tree level information is crucial for forest management with tree height being one of the most important parameters for dendrometric calculation. UAV processed data usually need to be annotated to point out the location or area of interest. One typical annotation is treetop, pointing at the highest elevation value. Since manual annotations can be time

consuming, especially for large area, numerous studies have attempted to automatized individual treetop detection. Tree crown shape and terrain complexity affect treetop detection (Nie *et al.*, 2019) since systematic distortion caused by slope terrain normalization reduces the performance of the treetop detection algorithm (Khosravipour *et al.*, 2015). Flight at a constant height in a slope increases treetops displacement during normalization. Several approaches including artificial intelligence such as convolutional neural networks (Xiao, Qin and Huang, 2020) has been used for treetop detection, but none has focused on treetop detection when following the slope.

The application of computer vision techniques, namely the Local Maxima Algorithm on the Canopy Height Model (CHM) (Diez *et al.*, 2020; Mohan *et al.*, 2021; Nguyen *et al.*, 2021; Thiel and Schmullius, no date) or on the Dense Point Cloud (DPC) to automatically detect treetops within a forest stand have been used in studies in mountainous terrain. However, in these cases the image collection was not done following the terrain and it is possible that the quality of the DPC and the CHM could have not reached their maximum potential as their heterogeneity within the surveyed area was not taken into consideration. Thus, the algorithm detecting treetops might have a good performance in some areas of the CHM but a poor performance in others (Mohan *et al.*, 2021). This issue is clearly observed in (Nguyen *et al.*, 2021), where co-dominant trees observed in the orthomosaic were not found in the CHM, mainly because of the lack of data in the DPC for lower trees. Thus, we hypothesized that DPCs generated from UAV-acquired images using TAF will improve the performance of the treetop detection algorithm, which in turn can have a positive impact on forest management of mountainous areas. Therefore, the aims of this study are 1. To compare the difference in the quality of DPC and CHM produced by a Mavic 2 Pro in a slope covered by fir trees using TAF, and 2. To evaluate the performance of two treetop detection algorithms on the CHM when the terrain is followed (TAF) and when it is not (NTAF).

## 2.2 Materials and Methods

### 2.2.1 Study site

We conducted this study in Zao mountains (Figure 2.1), a composite stratovolcano in southeastern Yamagata prefecture (140°24'39.224"E, 38°9'0.327"N) in a 20° slope covering an area of 3.8 ha. The fir stand in the slope has a density of 117 trees/ha and is dominated by mature Maries fir (*Abies mariesii*) trees mixed with deciduous broadleaves species (*Acer spp., Fagus crenata, Quercus mongolica, Sorbaria aorbofolia*). Fir is a highly valuable tree in Japan because of its obvious ecological function but mainly as a tourist attraction as they formed the famous 'Snow Monsters' in winter when they are covered completely by snow. In recent years, bark beetle attacks have seriously affected fir trees health (Leidemer *et al.*, 2022).

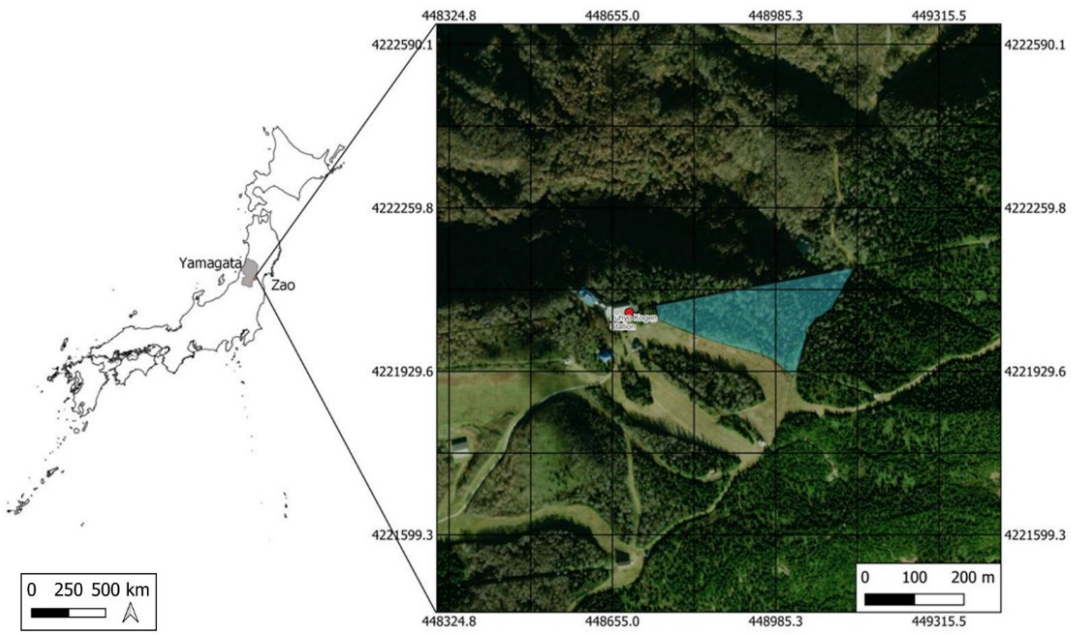


**Figure 2.1:** Location of the study site in Zao mountains next to Juhyo Kogen ropeway station. The fir trees are mixed with deciduous broadleaves species in the selected slope.

2.2. Unmanned Aerial Vehicles and flight plans

We collected the data using a Mavic 2 pro DJI quadcopter drone equipped with height definition RGB digital camera of 1inch CMOS 20 MP effective pixel. The camera L1D-20C of the Mavic 2 pro is equipped with 77 degree viewing angle lens, numerical shutter, and Hasselblad Natural Color Solution (HNCS) that reproduce good detail color (10-bit) for 5472 x 3648 image size. The pictures are georeferenced with drone on board positioning Global Navigation Satellite System; GPS and GLONASS.

A digital elevation model (DEM) is necessary to enable the UAVs to follow the terrain in slopes. For automated flight mission we used "Drone Deploy'' application, which in contrast to the original DJI application "DJI GS PRO" offer a terrain awareness function using an online Mapbox optimized data set based on NASA SRTM elevation grid.

Sets of RGB images were collected on October 5, in autumn, to better distinguish the spectral contrast of fir trees to the surrounding senescing colors of the deciduous trees. We flew two missions: using TAF and NTAF using the same parameters. The settings were, 90 m flying altitude and 85% front and side overlapping to create structure from motion (SfM) 3D models. This setting leads to a ground resolution of 1.98 and 2.75 cm and an average distance from the cameras to the sparse cloud points of 95.8 and 127 m along the slope respectively for TAF and NTAF, respectively. The height aboveground varied from 79.5 to 100.5 m for TAF and from 85.0 to 157.0 m for NTAF. We collected 281 to 285 images with a resolution of 5472 x 3648 pixels for each flight.

### 2.2.2 Image Analysis

DPC, DSM and Orthomosaics were generated for post-processing analysis tasks using Metashape Professional v1.7.4 (Agisoft LLC, Saint Petersburg, Russia). The DPC, a desegregation of images contained into a set of millions of points with high value of spatial

resolution (x, y, z), is the base of any form of digital images processed data. The site points density was assessed using DPC from both flights focusing on the same region of interest (clip by the same georeferenced polygon) after removing duplicated cloud points. DPC was normalized (Figure 2.2) using an execute command batch file run in LIDAR data analyze software FUSION (USDA Forest Service, USA) environment, following three standard steps (Ground filter, Grid-surface create and Clip Data) and smoothing parameters. We used the software Global mapper v21.1.0 (Blue Marble Geographics, USA), a cutting-edge GIS software to generate Elevation Grid base on nDPC (normalized DPC).

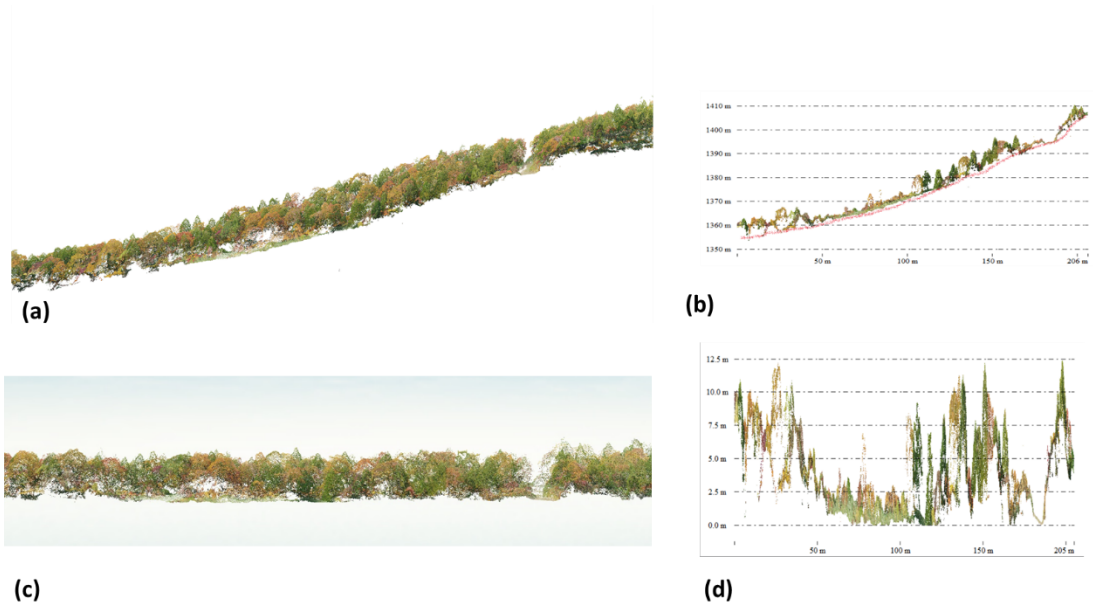


**Figure 2.2:** DPC normalization. (a) DPC; (b) filtered ground points based Digital Terrain Model ;(c) normalized points; (d) height aboveground.

The form of data that was used for more direct treetop detection in our study was CHM, a grayscale 2D aboveground elevation model obtained from the traditional difference (made in Fusion software) between the digital surface model (DSM) and the Digital Terrain Model (DTM).

The annotations (fir treetops) on the RGB orthomosaic were done on QGIS v3.22. The vectors shape files were rasterized and the output images were exported as PNG format. The generated CHM files were stored in tiff format and used as data input for the treetop detection algorithms. In the final step (data validation) the results of the treetop detection algorithms were compared to the manual annotations. (Figure 2.3).

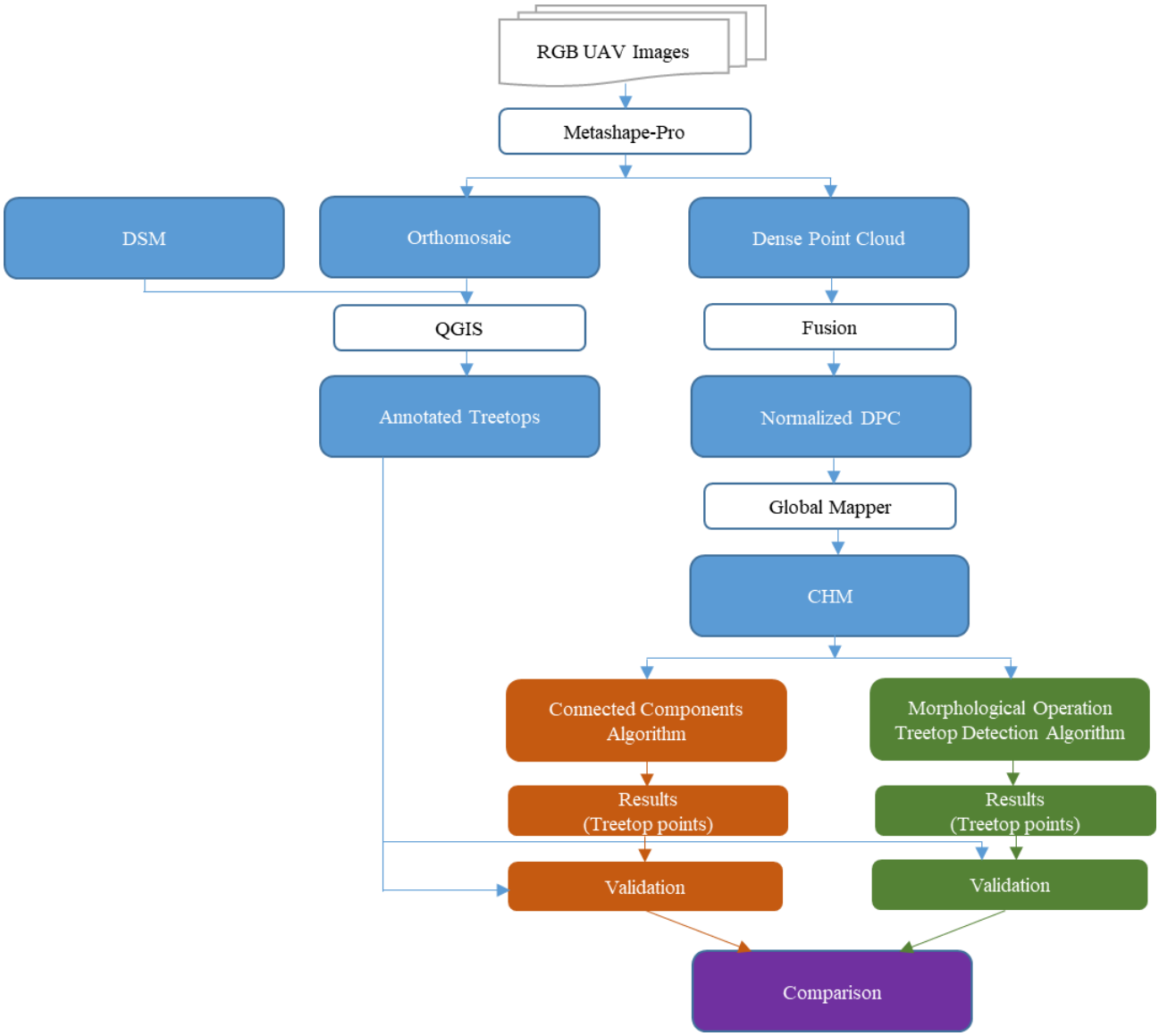


**Figure 2.3 :** Study workflow: processed data (blue), treetop detection algorithms process (orange and green); algorithm results comparison (purple) and commercial software used (white box).

### 2.2.3 Problem definition

The GSD varies along the slope, leading to heterogenous objects proportion and resolution. We divided our region of interest in three area (bottom, middle, upper) following a 10 m terrain contour line interval (Figure 2.4) in order to assess the UAV flying height aboveground fluctuation on data quality. The average GSD, when TAF was used, for the bottom, middle, upper area of the slope was 2.06, 1.96 and 1.99 cm/px with a range of 0,1 cm. In contrast, when NTAF was used the GSD in the same regions was 3.35, 2.91 and 2.49 cm/px with a range of 0.86 cm.

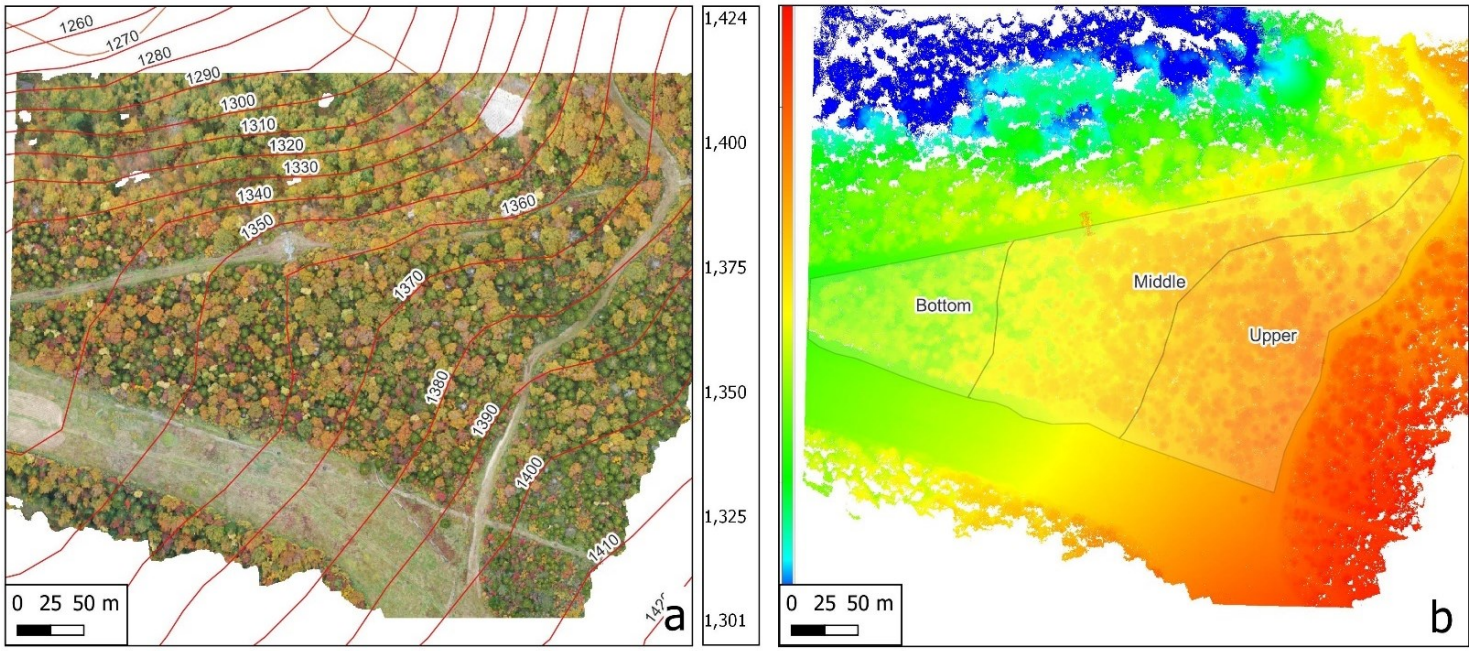


**Figure 2.4:** (a) 10-m contour line on the RGB orthomosaic of the study site and (b) the study site divided in three area related to their altitude: bottom (1330 m – 1350 m), middle (1350 m – 1370 m) and upper (1370 m – 1390 m).

### 2.2.4 Treetop Detection Algorithms

#### 2.2.4.1 Algorithm 1: Connected Components

In order to take full advantage of the precise data measurements represented in the CHM, a geotif data format with float components was used, allowing us to encode altitude values in millimeters. In order to detect treetops in the CHM, we used a modification of the algorithm

described in (Nguyen *et al.*, 2021) to adapt it to the higher quality of the CHMs used in the current work and for detecting only fir trees. Treetops can be formalized as local maxima in the 2.5D Canopy Surface discretized in the CHM files. Consequently, in this algorithm we performed a series of local searches (Figure 2.5), allowing us to minimize memory requirements by using a "sliding window approach".

Sliding Window Approach (Algorithm 1.1):

A bounding box for each CHM file was considered and a partition of this bounding box into fixed-side-length "s" "windows" was used. This process is analogous to picturing a single "s" side-length window that slides over the bounding box of the data set being processed (Figure 2.5). At each window position, we determined the local maxima corresponding to treetops, characterized as:

- Treetops are the highest points in their neighborhood.

- Treetops are surrounded by lower points forming the rest of the tree canopy, such that, when looked at from above, they would be separated from other treetops (at least in their upper part). Fir tree canopies are roughly conical so a set of fir trees seen from above can be pictured as a set of overlapping circles with the treetop at the center of the circles. As trees have different heights, it is difficult to automatically assess where each tree starts and where it ends

Treetop Determination (Algorithm 1.2)

For each position of the sliding window, we carefully considered the altitudes of the pixels in decreasing order and kept track of newly appearing trees. First, only a very narrow band of the pixels corresponding to the tallest trees in the window was considered. The pixels not in this band were set to 0. Consequently, in this initial band, only the topmost part of the tallest trees would appear as disjoint regions. We computed these regions (hereafter "connected

components") using a DAG labelling algorithm (Bolelli *et al.*, 2020) implemented in the "ConnectedComponentsWithStats" method of the OpenCV library. We ignored the connected components whose area was under a certain area threshold (minPoints) to avoid being misled by noise or possible image artifact. Several values were considered for this parameter to finally set a value of one fifth of the acceptable location error between treetops (Ɛ/5). We found the highest point in each of the components that was large enough and labeled it as a treetop. Whenever a new "large enough" connected component appeared, the highest value of that component in the CHM would be designated as a new treetop point would be assigned to it.

The process continued within the window until all pixel intensities were considered. At each new step the band of intensities considered was widened and the connected components in the resulting thresholded part of the CHM window was considered. For each connected component at each step, we would first determine whether or not it was a newly appearing component by checking whether any of the already detected treetops belonged to it. For newly appearing connected components, a new treetop would be detected in their highest point. Figure 2.5 presents a visual example of how the process develops. In the bottom left part of the figure (a), only the treetops are depicted as red points. In (b) to (e) we show how every time we widen the band of pixel being considered more treetops can be detected.

Once all the intensity values at one particular window location had been considered, the window was shifted to a new location. In order to avoid missing treetops "between windows", they had a small (5%) overlap among them.

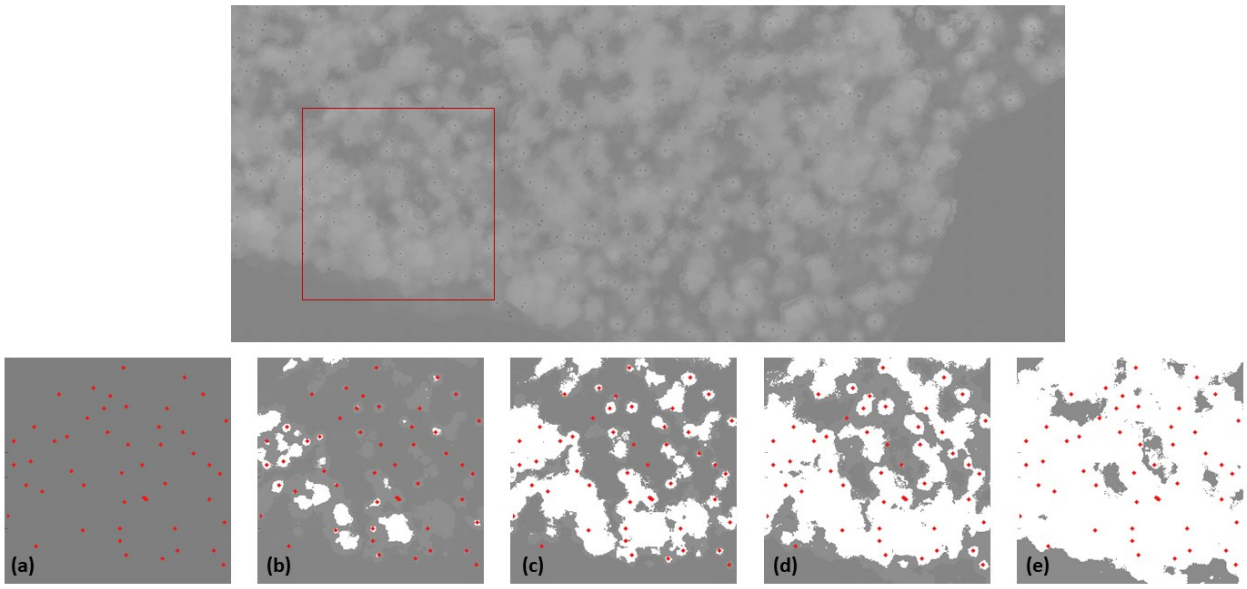


**Figure 2.5:** Fixed-side-length windows over the CHM sliding on different heights from above with (a) expert-annotated treetop positions then (b) initial tallest region appearing (c,d) new appearance and finally (e) the region's highest intensity are marked as treetops.

All code was implemented in the Python programming (pseudo code in Table 1) language (*Welcome to Python.org*, no date) using the OpenCV library (Bradski, 2000) and is available from the authors of the paper on demand.

**Table 1.** Algorithm 1 main step (Treetop Determination and Sliding Window) description as pseudo-code.

**Algorithm 1.1** Find_Tops_Connected_Components(CHM,minPoints,step)

**W** ← *AAWindows(CHM)* ▷ Set of axis-aligned "windows" sliding over the CHM.
*tops* ← ∅ ▷ "tops" initialised as empty list
**for** *w* ∈ ***W do***
*currentTop* ← *Process_Window(w, minPoints, step)* ▷ Find tops in this window
**end for**
**if** currentTops ≠ ∅ **then**
extend_list(tops,currentTops) ▷ Add tops to those of previous windows
**end if**
**return** tops

**Algorithm 1.2** Process_Window(w,minPoints,step)

*wTops* ← ∅ ▷ tops in this window initialised as empty list
*maxAlt* ← *Maximum(w)*
*expTH* ← *maxAlt* − *step* ▷ Explore altitude values from expTH upwards
**while** expTH > 0 **do**
*thWindow* ← *Threshold(w, expTH, maxAlt)* ▷ Delete altitudes < expTH
***C*** ← *ConnectedComponentsWithStats(thWindow* ▷ Detect Tree Top Candidates
**for** c ∈ **C do**
if Area(c)>minPoints **then** ▷ Component big enough to contain top
if NoTopInComponent(c,wTops) **then** ▷ No previous top is in this component
*top* ← *location(max(c))*
wTops.Append(top) ▷ Added new top to list of tops in the window
**end if**
**end if**
**end for**
*thWindow* ← *thWindow* − *step* ▷ Update loop condition
**end while**
**return** wTops

Changes with respect to [11]

In (Nguyen *et al.*, 2021) the algorithm made two passes over the CHM in order to account for a smaller trees that could be detected in the lower heights of the CHM. As we are only looking to detect fir trees, and not include deciduous trees we modified the algorithm to perform one single pass. Moreover, the shapes of fir trees are more clearly defined than those of deciduous trees, so the minimum number of points needed to consider a detected connected

component as a treetop was lowered and the rate at which new height values were added for consideration was increased.

### 1 2.2.4.2 Algorithm 2: Morphological operations

This algorithm used computer vision techniques to erase the borders (areas close to the floor) of local regions of the CHM. We used the fact that treetops are usually located in the middle of circular regions at high local altitude. By repeatedly erasing the borders of the local regions in the CHM we could isolate most of the trees and find its treetops (Figure 2.6). Morphological operators were used to isolate pixels that are at the maximum height of their local area and applied to the whole CHM.

The steps of the algorithm were as follows:

• First the lower altitude pixels were filtered out using global thresholding of the image.

• The resulting grayscale image was eroded using an elliptical Kernel to remove the borders of groups of pixels with the goal of separating trees.

• Then a Gaussian blur filter was used order to smooth individual tree canopies.

• Dilation was then used in the blurred image to make the highest pixels occupy a wider area.

• To ensure that no previously separated regions had been re-united, bit-wise comparison was used to compare the dilated and not dilated images.

After that, cycles of erosion + bit-wise AND were used to isolate smaller and smaller regions. This step had to be carried on with particular care as too many erosion operations may totally wipe out small trees.

• The groups of pixels left in the image are identified as treetop regions and the central point in each one was considered as a detected treetop.

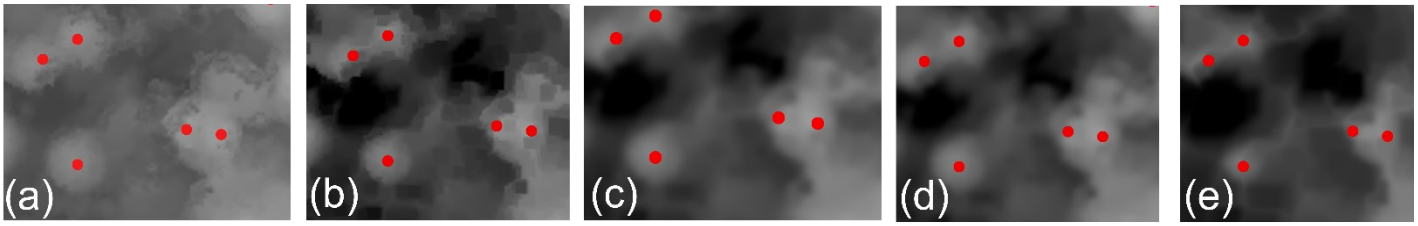


**Figure 2.6:** Image morphological operations cycle on (a) CHM with manual treetop annotation; (b) erosion, (c) Gaussian blur, (d) dilation and (e) erosion.

Table 2 presents a pseudo-code version of the algorithm. All code was implemented in the Python programming language [PYTHON] using the OpenCV library [OPENCV] and is available from the authors of the paper on demand. The different part of this algorithms was implemented using OpenCV's morphological operations mode that performs local bitwise operations by applying a small morphological kernel (in this case an elliptical one) at all possible positions of the CHM image.

**Table 2**. Algorithm 2 morphological operation and treetop detection pseudo code.

**Algorithm 2** Find_Tops_Morphological_Operators(CHM,minAlt,numIters)

```
thCHM←Threshold(CHM, minAlt,  Maximum(CHM)
▷ Pixels under minAlt become black
ero ← Erosion(thCHM, eKernel)          ▷ Elliptical kernel erosion (isolate regions)
blurr ← GaussianBlurr(ero, eKernel)    ▷ Gaussian Blurr (smooth canopies)
dil ← Dilation(blurr, eKernel)
comp ← (blurr > dil)
▷ Keep only pixels that have increased in value because of dilation
It ← 0
Im ← comp
while it < numIters do
newEro←Erosion(im, eKernel)
im = newEro  &  im
▷ Further isolate regions erosion + logical AND
it ← it + 1                    ▷ Update loop iterator
end while
```

2.6. Treetop detection validation

A series of validation metrics were calculated in order to assess the accuracy of the treetop detection algorithms The result of the algorithm was a set of 2D points where three metrics were applied to assess the effectiveness of automated treetop detection based on the expert annotation (ground truth point). The number of trees annotated on the orthomosaic was 464.

**Matched ground truth points percentage (m%):** the aim of this criterion is to check how many treetops were correctly detected. The mean fir tree crown radius from the study site orthomosaic was 2 m but we used different margins of error (1, 1.5,2 m) for a thorough validation. For the rest of the paper, we will refer to this margin of error also as "Ɛ" The points within the considered radius value threshold of a ground truth point were considered 'matched'.

**Repeated ground truth points percentage:** in this last step, we also computed the percentage of ground truth points that were matched more than once. This criterion indicated more thoroughly the source of the prediction overestimation. A high number indicated a

difficulty to separate individual treetops and a low number indicated erroneous points being detected in the outer parts of the tree canopies.

**Counting measure (cnt):** stands for the difference of trees present in the CHM "n", with the number of treetops detected "k" weighted over the number of trees cnt = (n−k) /consequently, negative values indicate that the algorithm overestimated the number of trees while positive values indicate underestimation.

Even though it would be possible to define a matched predicted point as a true positive prediction and an unmatched one as a false positive and use these labels to use well-established metrics such as sensitivity, specificity, F-score (Mohan *et al.*, 2017), this definition would not take into account multiple matchings from predicted points to ground truth points or vice-versa. Taking into account that tree counting is an important problem in our application scenarios, we decided to use the aforementioned measures (three criteria) that target broader possibilities of treetop counting.

## 2.3 Results

### 2.3.1 TAF vs NTAF datasets, qualitative evaluation

The orthomosaics made with images collected with TAF and NTAF showed different results concerning the details fir tree characteristics, mainly a deep view of tree canopies along the slope. When TAF was used, tree canopy area (lower branches) was clearer in the bottom area as well as in the upper area of the slope (Figure 2.7a). Instead, when NTAF was used the details of the lower tree layers within the fir stand, were missed at the bottom area of the slope, because of the higher GSD (Figure 2.7b). In general, tree canopies shape did not show any distortion after stitching images collected at different altitudes in order to assemble the orthomosaic when TAF was used. This is relevant because the treetop annotation might not be

done precisely in the actual center of the tree, where the canopy shape has been affected by the steepness of the slope.

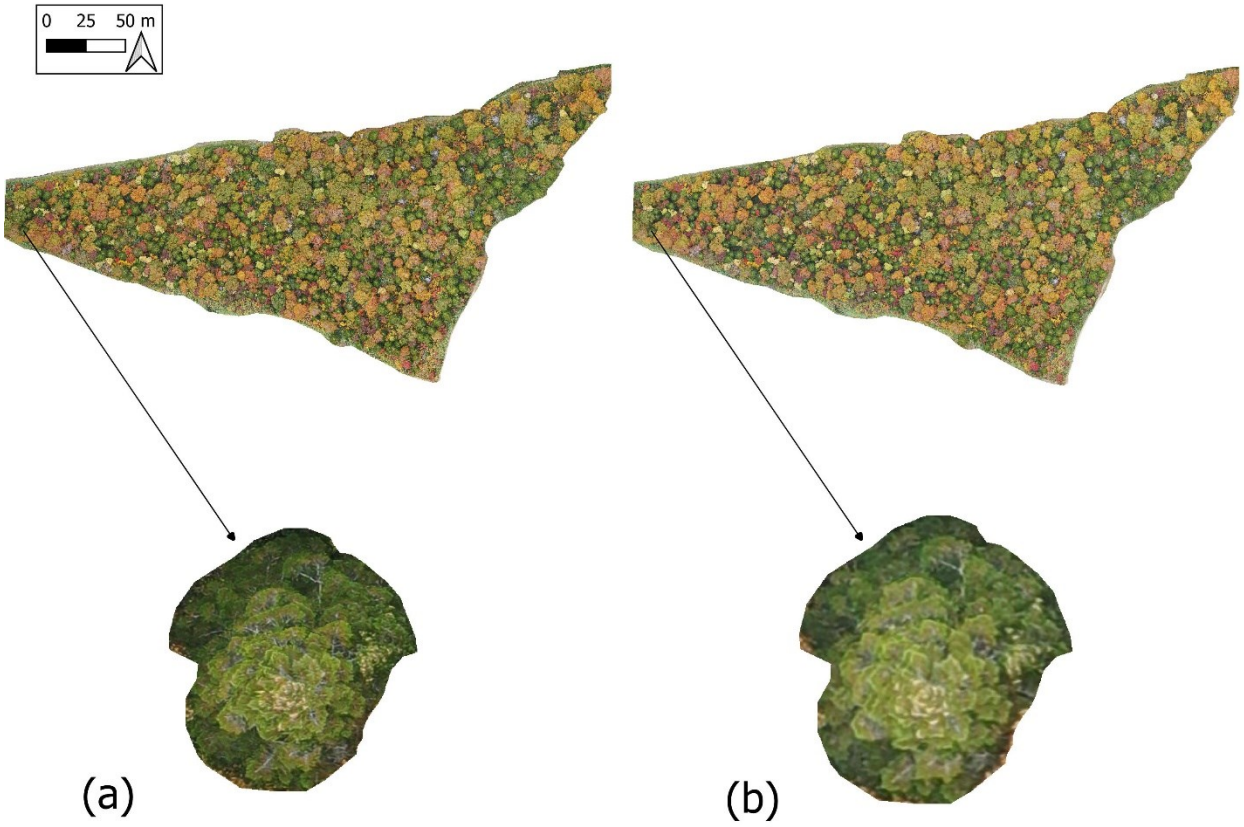


**Figure 2.7:** Region of interest and fir tree canopy difference in the bottom area of the orthomosaic; when using (a) TAF, lower branches and the shape are clearer and (b) when not, less details are visible.

### 2.3.2 Dense Point Clouds (DPC) and Canopy Height Model (CHM)

The Density of the DPC significantly increased and its points were distributed uniformly along the slope when TAF was used (Figure 2.8). The total number of points in the study site generated when using TAF was 15,099,519 and 8,599,946 when flying at a constant height (NTAF). The number of filtered ground points at the bottom and middle area were 38,1048 and 33,024 respectively, while when TAF was used the number of points were 747,184and

57,432, respectively. (Figure 2.8). In general, trees dimension along the slope when TAF was used was more homogeneous than when it was not used. There were no blank spots in the orthomosaic obtained with the TAF flight despite of using the commercially available SRTM.

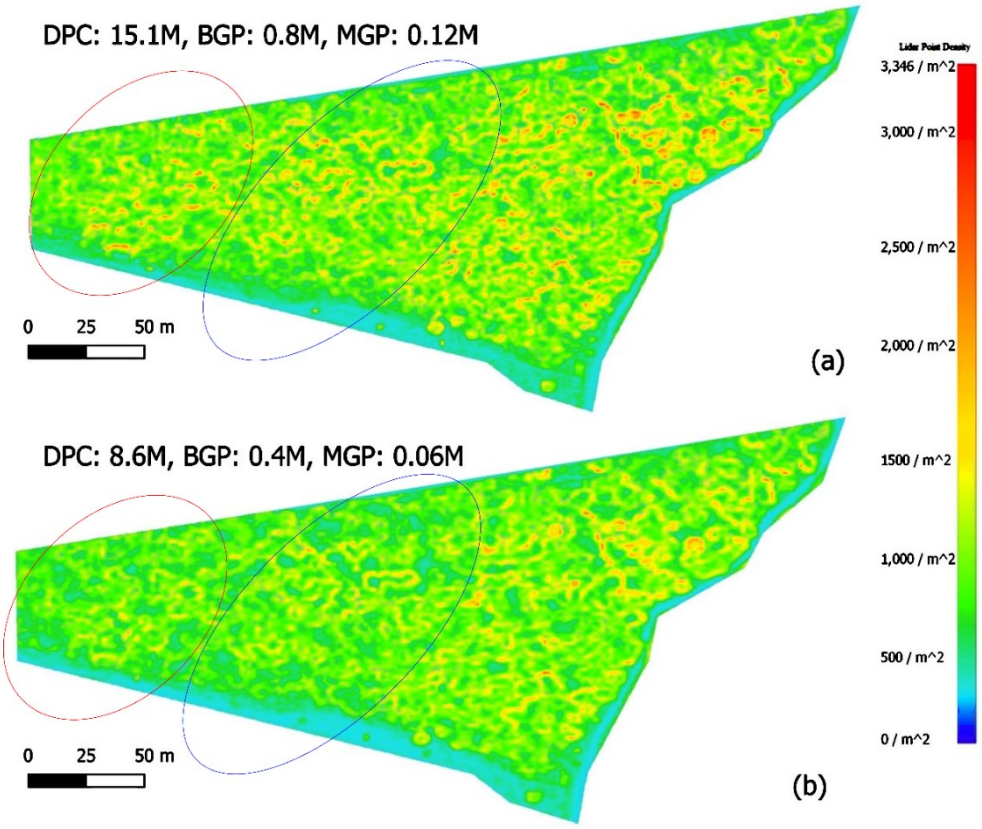


**Figure 2.8:**. Distribution of the DPC (a) when applying TAF and (b) NTAF. The difference in DPC Ground Point number in million (M), bottom area (red circle) Ground Points (BGP) and Middle area (blue circle) Ground Points (MGP) is significant when using (a) TAF and (b) NTAF.

### 2.3.3 Treetop detection

Considering margin of error=2m, (two meters between a predicted point and an annotated treetop) as an acceptable matching error, Algorithm 1 obtained results slightly close to 90% for both datasets reaching a maximum of 90.81 matching percentage using TAF and 89.91% for

NTAF, while Algorithm 2 detected about 81% of the existing points using TAF dataset and about 70% using NTAF dataset (Table 3). Algorithm 1 and Algorithm 2 show an increasing repeated percentage as the margin of error increasing and less repetition when using TAF. Algorithm 1 repeated 1.04% of matched point at Ɛ=1m when using TAF while Algorithm 2 show a maximum repetition of 7.17% when NTAF. This illustrates how by using TAF we can get predicted points that are closer to the ground truth points.

**Table.1:** Treetop detection validation. Results of the matching percentage and repeated percentage. This table shows the result of the two algorithms when using TAF and NTAF following three crowns radius parameters.

| Margin of Error | | 1m | 1.5m | 2m |
|---|---|---|---|---|
| Matching% | | | | |
| Algorithm 1 | TAF | 86.55 | 88.79 | 90.81 |
| (Connected Components) | NTAF | 81.8 | 87.5 | 89.91 |
| Algorithm 2 | TAF | 76.23 | 79.37 | 81.17 |
| (Morphological Operation) | NTAF | 62.06 | 68.2 | 70.39 |
| Repeated % | | | | |
| Algorithm 1 | TAF | 1.04 | 2.02 | 3.21 |
| (Connected Components) | NTAF | 1.07 | 4.51 | 6.59 |
| Algorithm 2 | TAF | 1.18 | 3.95 | 6.08 |
| (Morphological Operation) | NTAF | 1.77 | 4.82 | 7.17 |

The Counting measure (cnt) showed an overestimation on the number of detected treetop of up to 10% for Algorithm 1, while Algorithm 2 tended to underestimate the treetops. (Table 4).

**Table 2.** Difference between ground truth treetops and detected treetops (cnt), where positive values indicate detected treetop underestimation and negative values indicate overestimation

| | Count measure (cnt) | |
|---|---|---|
| Algorithm 1 (Connected Components) | TAF | -10.99 |
| | NTAF | -1.75 |
| Algorithm 2 (Morphological Operation) | TAF | 19.66 |
| | NTAF | 33.11 |

## 2.4 Discussion

UAV image collection presents a remarkable flexibility to adapt to environmental and topographical characteristics of the forest site that is the focus of investigation. Most of the UAV missions in the reviewed literature have focused on surveying the terrain rather than on the vegetation cover, and to our knowledge none has focused on the effect of the terrain on the forest characteristics obtained from orthomosaics. When the terrain is the main objective of a UAV mission, the optical axis of the camera is typically set oblique to the ground (Kozmus Trajkovski, Grigillo and Petrovič, 2020). However, since our focus was on the treetops distributed on a slope, we set the optical axis of the camera vertical (-90) to the ground since regardless of the slope angle, trees along the slopes had a vertical direction towards the camera. The results of using Mavic 2 Pro, one of the most affordable and versatile UAV in the market,

together with DroneDeploy software, allowed flights that followed the terrain with high precision, unlike the results found by (Pepe, Fregonese and Scaioni, 2018) who found that TAF flights were prone to create blank spots in the orthomosaic. Thus, the M2P flew smoothly along the slope, keeping a stable height and GSD, and spikes of altitude changes during flight were not observed as reported by (Kozmus Trajkovski, Grigillo and Petrovič, 2020)

From the point of view of forestry, the increase in the number of points in the DPC with TAF flights provide a more accurate depiction of single tree structure. The sharp increase in the number of points captured in the tree canopy should be taken with care because there is more duplicate information that was generated when processing the data. Nevertheless, the higher density of DPC is important not only important for treetop detection but also for accurate detection of tree canopy characteristics that can be used for the precise evaluation, for example, of forest health (Safonova *et al.*, 2019; Nguyen *et al.*, 2021) or forest fire disturbance (Aicardi *et al.*, 2016) or for the estimation of dendrometric parameters (Lisein *et al.*, 2013). This is especially relevant for fir forests in Zao Mountains in Japan, because as shown by (Leidemer *et al.*, 2022), the rate of single fir tree defoliation can be used as a proxy and the results of using TAF will contribute to a higher precision of tree canopy evaluation of the forest stand along the slope.

A higher feature number (denser DPC) decreases the 3D points triangle face network interpolation effect and therefore results in a better- balanced elevation grid (CHM). Additionally, more filtered ground points enhance the CHM calculation accuracy. Consequently, in this study, we were able to use CHMs (TAF case) that were much denser locally than in previous studies using UAVs to survey forest ecosystems where only NTAF has been used.

Two algorithms were used to perform automatic treetop detection on the CHMs using TAF and NTAF. Both Algorithm performed better when using TAF, as shown in Table 3. When predicted treetops were allowed to deviate no further than one meter (Ɛ = 1) from the ground truth treetops, Algorithm 1 detected 86.55%, 81.80% (TAF, NTAF) of the treetops while Algorithm 2 detected 76.23, 62.06% (TAF, NTAF). These numbers also indicate that the use of TAF facilitate the prediction of a larger number of treetops that are closer to the ground truth.

The percentage of matched points grew sharply for both algorithms when Ɛ was increased, especially for the TAF dataset. This is especially clear for Algorithm 2 that is less tailored to the current data. With Algorithm 1, we were able to reproduce the results of [11], specifically, 89.6% for healthy fir and 90.7% for sick fir trees when the margin of matching error 2 meters. In the current study only healthy fir trees were consider and algorithm 1 achieved 90.81% of matching. The results of Algorithm1 showed its ability to find a high number (81.8%) of close (1m) matches even for the NTAF dataset, proving that a dedicated algorithm can make up for some of the imprecision in the data. This higher matching quality is particularly clear for TAF data and is further illustrated by the percentage of predicted points that are matched to more than one real point. The percentage of repeated point increased with the margin of error (Ɛ) because having further matches also means that predicted treetops can be close enough to more than one ground truth treetop. However, in the case of Algorithm1 and TAF, there is a small increase that remained around 3% even for Ɛ=2m, while Algorithm 1 using NTAF dataset reach 6.59% repetition. The percentage of repetition for Algorithm 2 were over 6% for both datasets (TAF and NTAF).

Algorithm1 was much more sensitive to height variations in the CHM and, thus missed fewer points. This came at the cost of sometimes detecting false treetops from irregularities in the canopies of fir trees or spurious elevations in the lower part of the crowns produced by

nearby deciduous trees. Our results showed how this algorithm predicted 11% of extra treetops. Algorithm 2 operated by smoothing out the boundaries of tree crown but appeared either to small trees or failed to separate groups of trees Thus, Algorithm 2 tended to underestimate the number of treetops present and missed some of the existing ones. This is expressed by the positive values in the "point diff" criterion (Table 4).

## 2.3 Conclusion

In this work we have studied the effect that TAF has on the quality of UAV-acquired data. Our data was produced using an inexpensive UAV and publicly available elevation data. We have provided qualitative and quantitative evaluation of two Algorithms using TAF and NTAF datasets to automatically detect treetops. The results show that even in mountainous terrain conditions as that presented in this study, most of the existing treetops were detected

The results showed that Algorithm 1 was able to detect 86.55% of treetops for TAF and 81.80% for NTAF when only 1 m margin of error was set. Thus, fewer points matched more than once the ground truth treetop when TAF was used. Treetop detection was improved by 14% when using Algorithm 2 and TAF (76.23%) than when using NTAF (62.06%) for 1 m margin of error. Thus, our study showed that using TAF on the acquisition of UAV data decrease matching repetition, improve treetop detection by providing better CHM.

# Chapter 3: Treetop Detection in complex slope using UAV Terrain Awareness Function and self-generated Digital Elevation Model

## 3.1 Introduction

Structure from motion (SfM) photogrammetry applied on UAV acquired images hhas proved to be useful for forestry investigation (Iglhaut *et al.*, 2019). SfM provide high resolution three-dimension (3D) data allowing dendrometric measurement (Rodríguez-Puerta *et al.*, 2022) while spectral signature inform about health condition (Gupta and Pandey, 2021). Thus, UAVs are becoming standard platforms for remote sensing captors.

UAV offer good operation flexibility allowing high precision of real time manual and automatic flights. UAV manufacturers as well as software developers are continuously improving the navigation performance including position and orientation sensors. at present, UAVs can include environmental constrain parameter in the flight plan such as terrain relief.

Global data server like SRTM (NASA) is used as base information for terrain awareness flying mode which allows the UAVs to fly following terrain, but such a data have usually coarse resolution and low positioning precision. Positioning error and low resolution can produce malfunction in the UAVs during the flight, increasing crashing risk and affect the final data quality. Some drone mapping software make an optimal use of global data by calibrating the course base on the real field height above ground planned value (DroneDeploy) instead of making use of row altitude above sea level value (DJI GS RTK). Using a self-build digital surface model (DSM) of a given slope for terrain awareness mission, the UAV perform better (Kozmus Trajkovski, Grigillo and Petrovič, 2020).

Computer vision techniques based on local maxima have been widely used for treetop detection (Safonova *et al.*, 2019; Rodríguez-Puerta *et al.*, 2022; Thiel and Schmullius, 2016). Using terrain awareness function produce homogeneous resolution in the images collected along the slope and a better canopy high model (Gonroudobou *et al.*, 2022). Treetop detection

in mildly sharp slope using algorithm  show slight improvement when terrain awareness function (TAF) is used than when it is not (Gonroudobou *et al.*, 2022).

In this chapter we make case that using TAF base on self-generated very high-resolution DSM in very steep and complex terrain will show significant treetop detection improvement. Thus, objective of this  study is to evaluate the performance of treetop detection algorithms on the CHM when the terrain is followed (TAF) and when it is not (NTAF).

## 3.2 Materials and Methods

### 3.2.1 Study site

We conducted this study at Yamagata University Research Forest (N38° 32′, E139° 51′; m a.s.l.) in the Asahi Mountains in Yamagata prefecture, Japan (Figure 3.1).

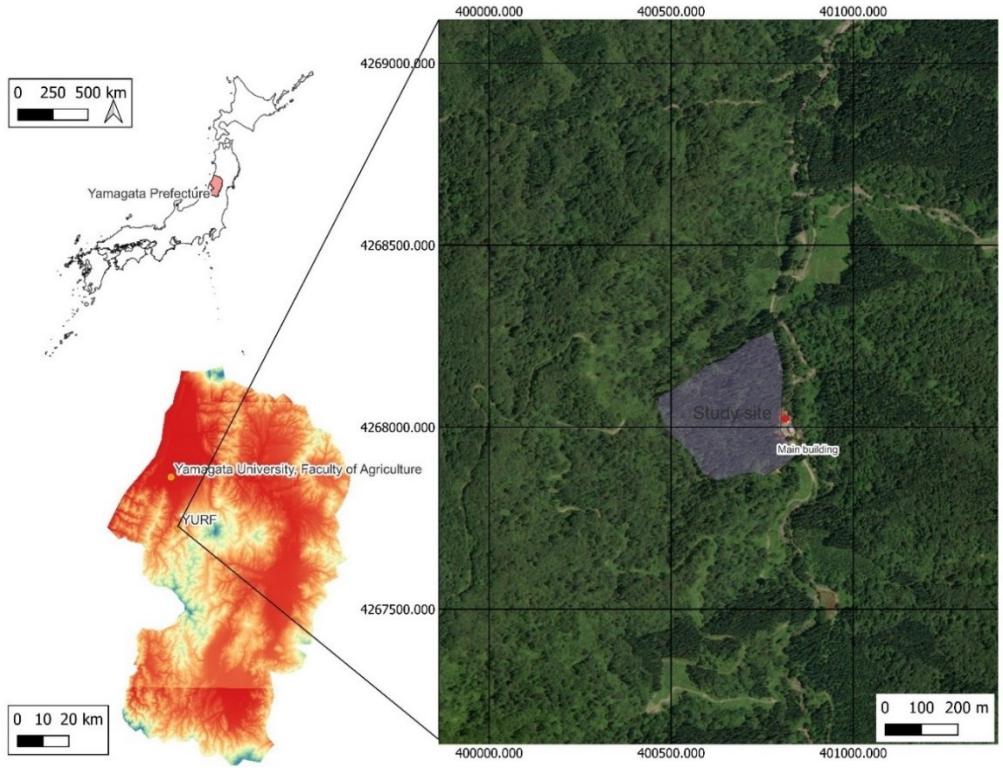


**Figure 3.1:** Location of the study site in Yamagata University research forest next to a building.

The region of interest is mature cedar tree plantation over 12 ha ranging from 280 to 440 m above sea level (Figures 3.2) corresponding to a 28-degree slope (Figure 3.3).

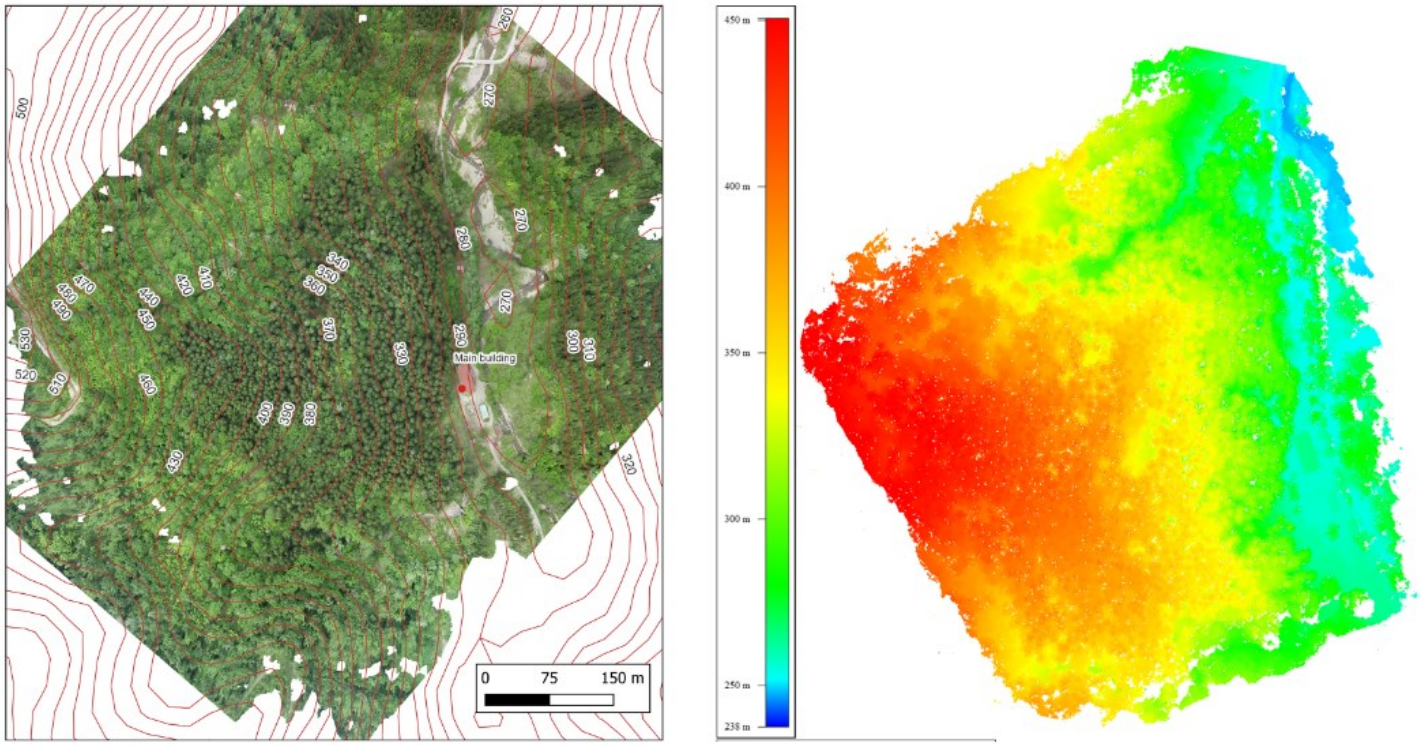


**Figure 3.2:** Study site slope

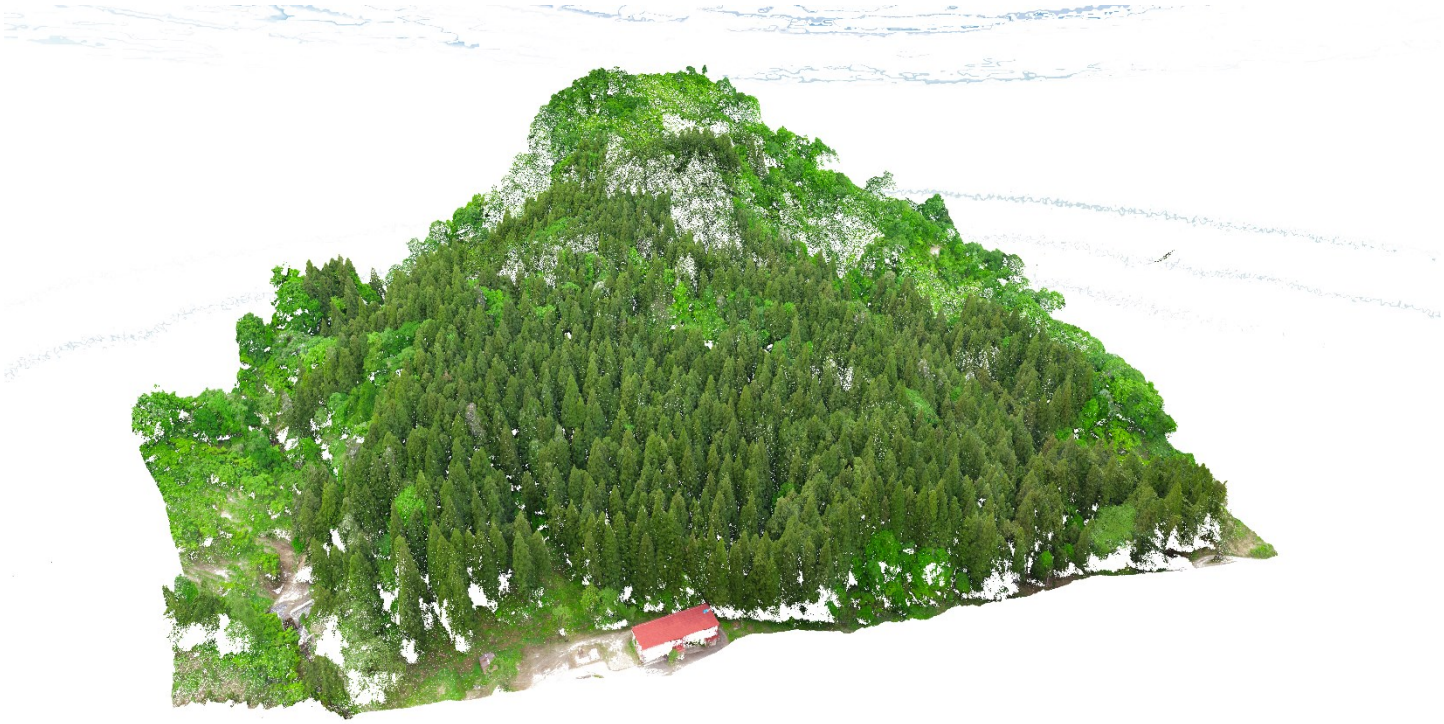

**Figure 3.3:** Study site 3D model illustrating the relief

### 3.2.2 Drone image collection and data processing

We collected the data using DJI quadcopter drone Phantom 4 RTK equipped with high-definition Red-Green-Blue digital camera of ‘’1 CMOS 20 MP effective pixel. The camera is equipped with a mechanical shutter, 84 degree viewing angle lens, 8-bit color and 5472 x 3648 image size allowing good area covering on one shot.

The images are georeferenced with on board positioning Global Navigation Satellite System multi-frequency multisystem precision Real Time Kinematic (RTK) module providing centimeter level positioning data.

The mission was planned using “DJI GS RTK” (DJI Inc., Shenzhen, China) a phantom 4 RTK dedicated flight planning application allowing a Terrain Awareness flying mode based on user provided Digital Surface Model DSM (Figure 3.4 ) imported in the remote control via a Micro SD.

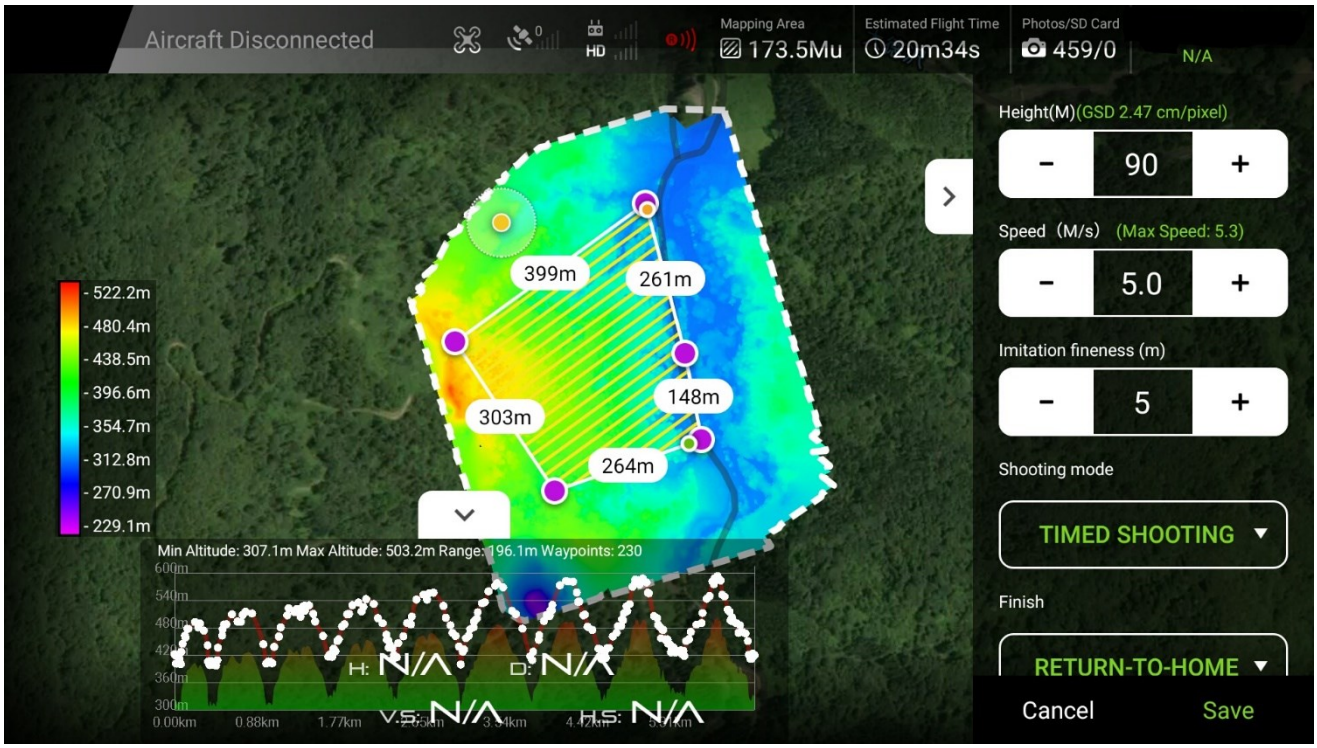


**Figure 3.4:** DJI GS RTK interface of terrain awareness function mission plan

UAV self-generated DSM were used.

Sets of 686 images were collected and pre-process in Metashape (Agisoft LLC, Saint Petersburg, Russia) following five step workflows (Figure 3.5).

| | |
|---|---|
| Alignment parameters | |
| Accuracy | Medium |
| Generic pre-selection | Yes |
| Reference pre-selection | Source |
| Key point limit | 100,000 |
| Key point limit per Mpx | 1,000 |
| Tie point limit | 100,000 |
| Exclude stationary tie points | Yes |
| Guided image matching | No |
| Adaptive camera model fitting | No |
| Point Cloud | |
| Points | 2,221,643 of 2,427,572 |
| RMS reprojection error | 0.140953 (1.30297 pix) |
| Max reprojection error | 0.429459 (58.7965 pix) |
| Mean key point size | 7.38088 pix |
| Point colors | 3 bands, uint8 |
| Key points | No |
| Average tie point multiplicity | 4.07905 |
| Texturing parameters | |
| Mapping mode | Generic |
| Blending mode | Mosaic |
| Texture size | 4,096 |
| Enable hole filling | Yes |
| Enable ghosting filter | Yes |
| DEM | |
| Size | 3,834 x 4,206 |
| Coordinate system | WGS 84 (EPSG:4326) |
| Reconstruction parameters | |
| Source data | Dense cloud |
| Interpolation | Enabled |
| Orthomosaic | |
| Size | 14,676 x 16,269 |
| Coordinate system | WGS 84 (EPSG:4326) |
| Colors | 3 bands, uint8 |
| Reconstruction parameters | |
| Blending mode | Mosaic |
| Surface | Mesh |
| Enable hole filling | Yes |

**Figure 3.5:** Metashape professional edition image processing report

Dense Point Clouds (DPC), Digital Surface Model (DSM) and orthomosaics were generated. The DPC were normalized (Figure 3.6) and the canopy height model was created as indicated in Gonroudobou *et al.*, (2022).


**Figure 3.6:** DPC normalization (difference between digital surface model and digital terrain model)

ArcGIS pro (Esri, Redlands, California, United States) software were used for orthomosaics annotation and the vector files were set as raster ("vector to raster" tool) then exported as 2-bit color depth as .png format. GIMP software was used for manual treetops binary mask creation.

### 3.2.3 Treetop detection

In order to automatically detect treetops, we used morphological operation algorithm as in chapter 2. This algorithm is based on computer vision techniques and apply a series of image operation (erosion, dilation and blur) the CHM in order to highlight local data (local maxima).

By repeatedly erasing the borders of the local regions in the CHM it is possible to isolate most of the canopy and find its tops.

Morphological operators were used to isolate pixels that are at the maximum height of their local area and applied to the whole CHM. The steps of the algorithm were as follows:

Filter out low heights.

•Erode the image to removes the border of any group of pixels.

•Blur the image applying Gaussian blur.

•Dilate the blurred image to makes the highest pixels occupy a wider area.

•Compare the dilated image and the image before dilation, allowing the pixels that were grouped up to be isolated.

•Erode the image again and make another comparison.

•Perform an AND operation between the images before and after applying erosion.

This last couple of steps can be repeated several times to increase the accuracy of the results, however it may cause some groups of pixels that are too small to be erased, which might imply a loss of important data.

•Find all the group of pixels left in the image. After the operations previously made all the remaining groups of pixels was the highest points on the image.

Treetop detection validation

To assess the accuracy of the treetop detection algorithm, three validation parameter was calculated. Based on the algorithms result as 2D (x,y) dot map, we used three metric criteria as in chapter 2 to compare with a manual annotation (ground truth point) the effectiveness of the automated treetop detection.

**Matched ground truth points percentage (m%):** the aim of this criterion is to check how many treetops were correctly detected. The mean cedar tree crow radius from the study site orthomosaic was 2.5m (epsilon 15 and 17 respectively for TAF and NTAF). Thus, we consider as matched point the detected point within 2.5m.

**Counting measure (cnt):** is the difference between ground truth point "n" and treetops detected "k" cnt = n−k.

**Repeated ground truth points percentage:** We computed the percentage of ground truth points that were matched more than once.

## 3.3 Result

### 3.3.1 TAF vs. NTAF Datasets—Qualitative Evaluation

The orthomosaics when using TAF showed a more detailed image of individual tree canopies along the slope than when NTAF was used (Figure 3.7 ).

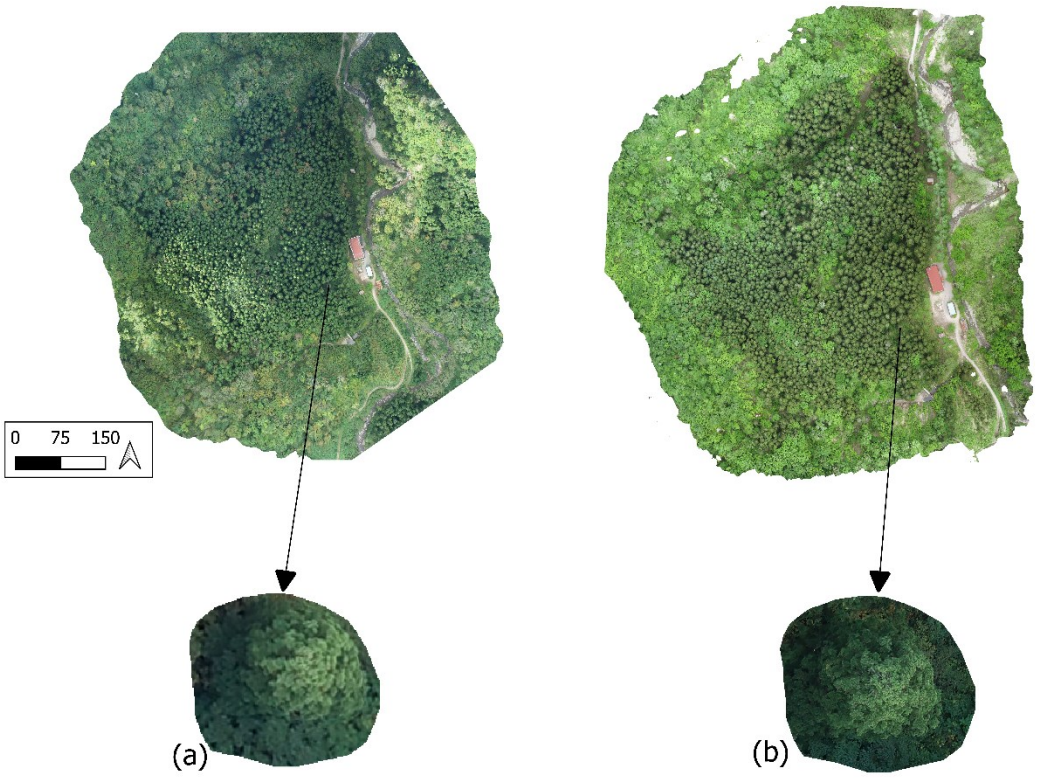


**Figure 3.7:** bottom area tree show (a)lower resolution when NTAF than (b) when TAF was used

### 3.3.2 Treetop Detection

Considering that detected treetop should be within the tree canopy area , a margin of error of 2.5 m (2.5 meters between a predicted point and annotated treetop) corresponding to the mean canopy ray was set as an acceptable matching error.

Morphological operation Algorithm obtained results over 90% for both datasets when the margins error was 2.5m. The matching percentage varied from 83.69 to 93.95% and from 83.27 to 91.42 respectively when TAF and NTAF. In both case the matching percentage was positively correlated to the margin of error. The same result was observed for the repeated percentage.

Table 3 Treetop detection validation. Results of the matching percentage and repeated percentage. This table shows the result when using TAF and NTAF following three crowns radius parameters.

| Margin of Error | 1.5m | 2m | 2.5m |
|---|---|---|---|
| Matching % | | | |
| TAF | 83.69 | 88.82 | 93.95 |
| NTAF | 83.27 | 87.79 | 91.42 |
| Repeated % | | | |
| TAF | 1.71 | 4.95 | 5.92 |
| NTAF | 3.20 | 8.40 | 12.57 |

The Counting measure (cnt) showed an overestimation for both data set on the number of detected treetops of up to 15.30 percente.

Table 4 Difference between ground truth treetops and detected treetops (cnt), where positive values indicate detected treetop underestimation and negative values indicate overestimation

| Count measure (cnt) | |
|---|---|
| TAF | 10.79 |
| NTAF | 15.30 |

## 3.4 Discussion

In the previous chapter we studied the effect that TAF has on the quality of UAV-acquired data. Our data were produced using available global elevation data. We assessed two algorithms using TAF and NTAF datasets for treetop detection. Our study showed that treetop detection was more precise when TAF was used by decreasing matching repetition Considering that flying following terrain using our own digital surface model may improve the accuracy of the UAV course (Kozmus Trajkovski, Grigillo and Petrovič, 2020) and that a more steep and irregular terrain could show better improvement, we conducted the current study filling up all those possibility.

For this study, we assess the improvement of morphological operation, a general computer vision technique base approached that simplify the local data (local maxima) then point out the maxima. This algorithm was easier to run in such a big study site (12ha) compare the tailored "connected component" used in the previous chapter. Morphological operation algorithm process might delete small local or count a group of trees too close as one ; that result to an underestimation of detected treetop compare to the ground truth point as shown in table 4. This observation was conform to the previous chapter result (Gonroudobou *et al.*, 2022).

The percentage of matched points grew for both data set (TAF and NTAF) when the margin of error was increased but TAF remained higher. Detected treetop percentage was 83.69, 88.82 and 93.95% when TAF was used, while 83.27, 87.79 and 91.42% was obtained for NTAF at 1.5, 2.0 and 2.5 m margin error respectively. In all cases the use of TAF improved the detection. In contrast with the result from the previous chapter we found better performance of the algorithm using both data set and lower improvement using TAF. The improvement obtained by Gonroudobou et al (2022) was 14.17 and 10.78%, while in the current study we found 0.42 and 2.53% respectively for the minimum and the maximum margin error. That could be explain

by the fact that this study site is covered by a planted tree with more or less homogeneous tree size and in average bigger than in the study chosen in chapter 1. Phantom 4 RTK smooth and precise mission course due to the geocoordinate correction and additional object correction lens into the UAV camera could have reduce the effect of the slope on the collected images.

The percentage of repeated points increased with the margin of error (ε), because having further matches also means that predicted treetops can be close enough to more than one ground-truth treetop

## 3.5 Conclusion

We assess the performance of treetop detection algorithm when using TAF base on self-generated DSM and when not (NTAF) for UAV data acquisition data. Our study site was a mountainous complex terrain.

The result show that we were able to detect 93.95% of treetops for TAF and 91.42% for the NTAF when 2.5m margin of error was set.Our study showed that using the TAF on the acquisition of UAV data decreased matching repetition and even in highly sharp slop terrain the improvement was not significant.

# Chapter 4: Scaling up from tree to forest stand Nitrogen based on UAV acquired image and field measurements

## 4.1 Introduction

Remote sensing for forest ecosystems investigation have been widely use in the last decade. The implementation of most of arial based approached are costly and usually required heavy equipment. The biggest issue being the support for various sensor ; the support such as big aircraft are used. Satellite imagery provide good alternative with moderately high resolution of data. However recent UAV technology available for the civilian market and powerful compact sensor open unlimited possibilities for science application offering good operation flexibility, cost efficiency and very high resolution and temporal data.

Traditional forest scientific research is based on human power and time-consuming field work that provide limited scale information. New technologies provide reliable information but this field is in building, required field work for data validation and are still limited mainly for biophysiological investigation. Even through field work for data validation seem to be conducted by the traditional way it is less demanding and is assumed as part of remote sensing methodology. Thus, there is a gap between the two methodologies, each one of them show advantages and disadvantages: traditional forest observation provides excellent in-situ information while remotely sensed provide larger scale high resolution temporal data (Fleming, Wang and McRoberts, 2015). A combine methodology between traditional field work and remote sensing is not new though, several studies have attempted to take advantage of remotely sense data resolution for scaling up local forest data to stand level using remotely sensed information.

Good resolution for forest global information has always been one of the main focuses of scientist (Davies *et al.*, 2021). Scaling up local data to landscape or regional level have been attempted multiple times ((Čermák, Kučera and Nadezhdina, 2004; Lecointe *et al.*, 2006)). Tree spatiality has been used to scale up plot to forest stand information since the interaction

mechanism is link to the forest ecosystem structure (Smith and Urban, 1988). Plot data to inventory vegetation map (Čermák, Kučera and Nadezhdina, 2004; Lecointe *et al.*, 2006), plot to UAV imagery map (Geng *et al.*, 2021), plot data to satellite imagery map (Fleming, Wang and McRoberts, 2015; Calders *et al.*, 2020), UAV imagery map to satellite image map (Kattenborn *et al.*, 2019) or laboratory simulation to UAV imagery map (Zarco-Tejada *et al.*, 2001) accurate scaling up issue has been addressed.

Nitrogen (N) is a key element in every ecosystem, (Vitousek *et al.*, 2002) vital for plant biochemical and physiological function controlling plant growth and productivity (Leghari *et al.*, 2016). In recent years, the analysis of natural abundance of nitrogen stable isotopes in plant tissues have proved to be immensely useful for nutrients tracking (Lopez Caceres *et al.*, 2018; Seidel *et al.*, 2019; Murata *et al.*, 2022). Stable isotopes has been used effectively to trace mycorrhizal fungi symbiose in mainly nitrogen limited environment (Hobbie and Hobbie, 2008) and recent abundant anthropogenic nitrogen deposition in natural ecosystem (Holtgrieve *et al.*, 2011). Intra-plant nitrogen recycling (Seidel *et al.*, 2019) litter contribution to the ecosystem cycle (Yang, Deng and Zhang, 2007) and many other processes. Nitrogen is one of the most important elements to track in other to understand forest ecosystem response to climate change (Kahmen *et al.*, 2006; Reed, Cleveland and Townsend, 2011). In mixed forest the nitrogen cycle of individual tree is even more complex and poorly understood.

In this chapter we intend using very high-resolution UAV acquired images to establish measured leaves Nitrogen Isotope $\delta^{15}N$ and content N value map of four trees species to the stand level.

## 4.2 Material and Methods

### 4.2.1 Study site

We conducted this study at Yamagata University Research Forest (N38° 32′, E139° 51′; 265 m a.s.l.) in Shonai area in north-eastern Japan along the Japanese Sea side in Yamagata Prefecture (Figure 4.1). The climate is humid with an annual mean temperature of 9.7 °C. the heavy precipitation about 3000 mm of annual precipitation approximately 50% snow (~3m). The area is mountainous with an average slope ranging from 20 to 40 ° and the soil is mainly cambisol . The main species that distributes in the Forest Research Center are beech (Fagus crenata), Japanese Cedar (*Cryptomeria japonica*), hoonoki (*Magnolia hypoleuca*), oak (*Qercus mongolica* var. grosseserrata), Larch (*Larix kaempferi*) and other minor species. We focused on mixed forest between 580 m to 670 m a.s.l over 3.56 ha.

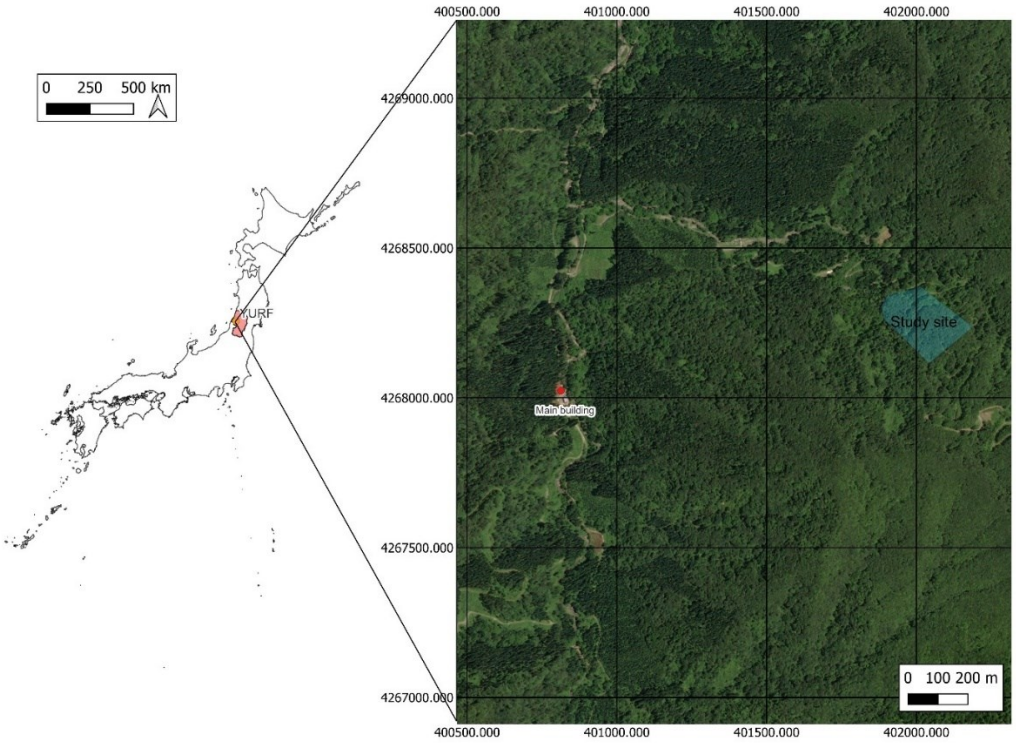


Figure 4.1: Study site at Yamagata University research forest in Asahi Mountain

### 4.2.2 Trees species Nitrogen measuring.

More than two third of Japan is covered by forests with 40% are platation. Japan climate have high variability  from the sub-tropical zone in Okinawa to the sub-frigid zone in Hokkaido and strongly monsoons. The monsoons from the continent bring bitter coldness to the northern region from November to March, and the regions facing the Sea of Japan experience heavy snowfall.

**Larch**

Native to most of the cooler temperate north hemisphere, Larche

(Figure 4.2) is one of the rare deciduous conifers in the genius *Larix* of the family Pinacea. Larch shed their needles leave in late autumn. Japanese Larch, *Larix keampferi,* is native to central and northern Japan. This species has been planted to Hokkaido after Meiji 30s and is found from central to northern Japan. In the Composition of Forest Ecosystems by Dominant Tree Species larch only occupyies 3% all planted (Japan Forestry Agency, 2019) . Japanese larch can grow over 50 m and withstand low soil fertility conditions.

Figure 4.2: single Larch tree drone view in summer (left) and autumn (right)

**Oak**

Oak (Figure 4.3) in *Quercus* genus of the family Fagaceae is one of the most common deciduous broad leaves tree species in the northern hemisphere. Japan count four native species *Q. serrata* Thunb. ex Murray, *Q. mongolica* Fisch. ex Ledeb. var. crispula (Blume) Ohashi, *Q. dentata* Thunb. ex Murray, and *Q. aliena* Blume (Kanno *et al.*, 2004). In Japan, *Quercus mongolica* is distributed almost all over Japan. mizunara in Japanese, oak can become giant trees.

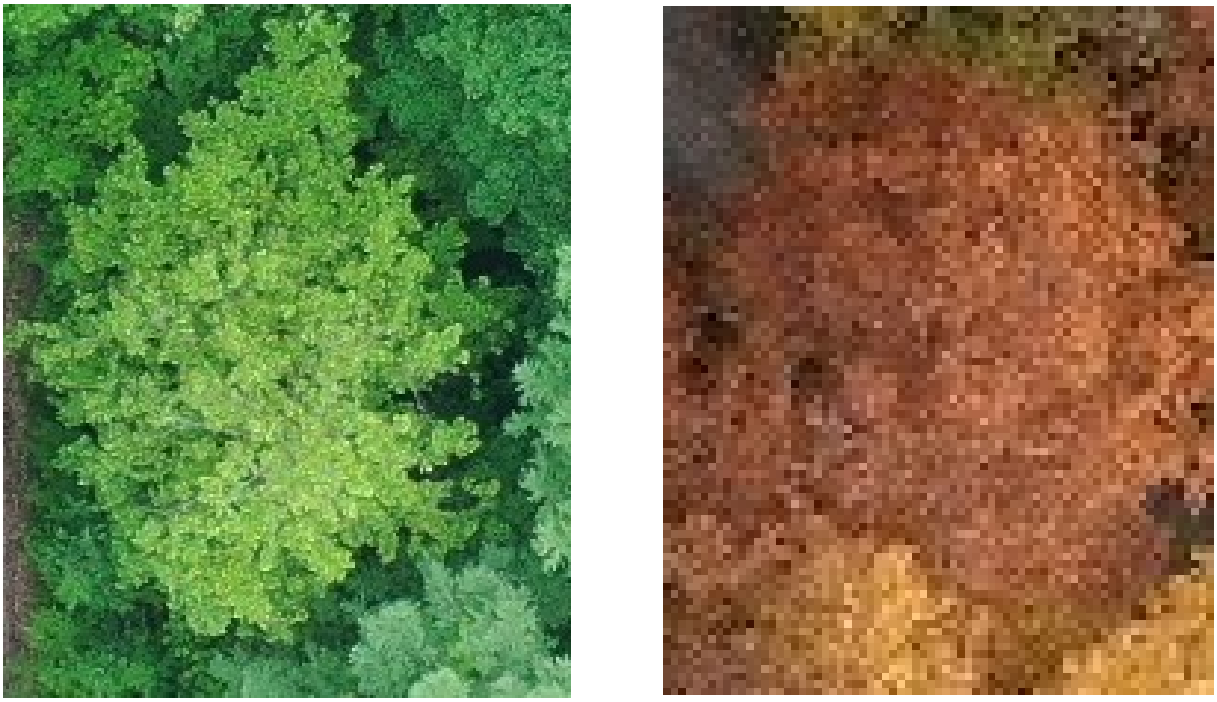

Figure 4.3: single oak tree drone view in summer (left) and autumn (right)

**Beech**

Native to temperate Europe, Asia and North America, Beech (Figure 4.4) in Fagus genus is a broadleaves deciduous trees in the family Fagaceae. Japanese Beech *Fagus crenata* is one of the country main species distributed from Kyushu to Kuromatsunai in the southern part of Shiribeshi Subprefecture (Hokkaido) where beech tree has been designated a natural treasure (Tateishi *et al.*, 2010). Buna in Japanese *F. crenata* has aslow growth the first 20 years but later can grow very tall.

Figure 4.4: single oak tree UAV view in summer (left) and autumn (right)

**Maple**

Known as kaede in Japan, maple trees are deciduous trees and shrubs belonging to Acer genus classed in the family Sapindaceae. Maple is a various group with over 100 species (Kikuchi *et al.*, 2009) mainly native to Asia. Maple is found basically in mountainous area and can grow more 12 m.

**Isotopic analysis**

Mature and isolated (to avoid surrounded tree effect on isotopic signal) Larche, Oak, Maple and Beech leaves were sample with three repetitions. After drying in the oven at 70 degrees

during 48 hours the sample were weight (5 mg) and prepared in aluminum thin cup for nitrogen analysis. The analysis was done using mass spectrometer.

### 4.2.3 UAV imagery collection and pre-processing

Sets of images were collected using two commercial drones equipped with Digital RGB camera in summer (DJI Mavic 2 Pro) and autumn (DJI Phantom 4 RTK). The automatic flights were planned using DroneDeploy for Mavic2Pro and DJI GS RTK (DJI Inc., Shenzhen, China) for Phantom4RTK. The drone flew at constant height and following terrain relief at 80 m and 90 m for 1.8 and 3 cm ground sampling distance respectively for Mavic2Pro and Phantom 4 RTK.

The images were pre-processed in Metashape (Agisoft LLC, Saint Petersburg, Russia) following batch process

Orthomosaic and Digital Elevation Model (DEM) were exported as .tif format using UTM Zone 54N projection.

### 4.2.4 Data processing.

Pre-processed data (orthomosaics) treetop was annotated on point feature shape file using ArcGIS Pro (Esri, Redlands, California, United States) on both summer and autumn orthomosaic after aligning Mavic2pro acquired orthomosaic on Phantom4RTK orthomosaic (RTK being more accurate). In ArcGIS Pro, 3 m square graphic buffer were created using treetop points for summer and autumn orthomosaic. Two data set of tree patches were created using ”Split raster” tool. In order to identify tree species a python program set as an executable (to avoid code manipulation mistake) was use to display side by side (Figure 4.5) same tree summer and autumn patches (to facilitate species recognition) and right defined species key were push for the classification. The program goes through all the patches and generate a text

result showing each specie and the tree id belonging to that category. The ids are then used to select (‘’select by attribute ‘’) the same species trees and the right value etiquette were set.

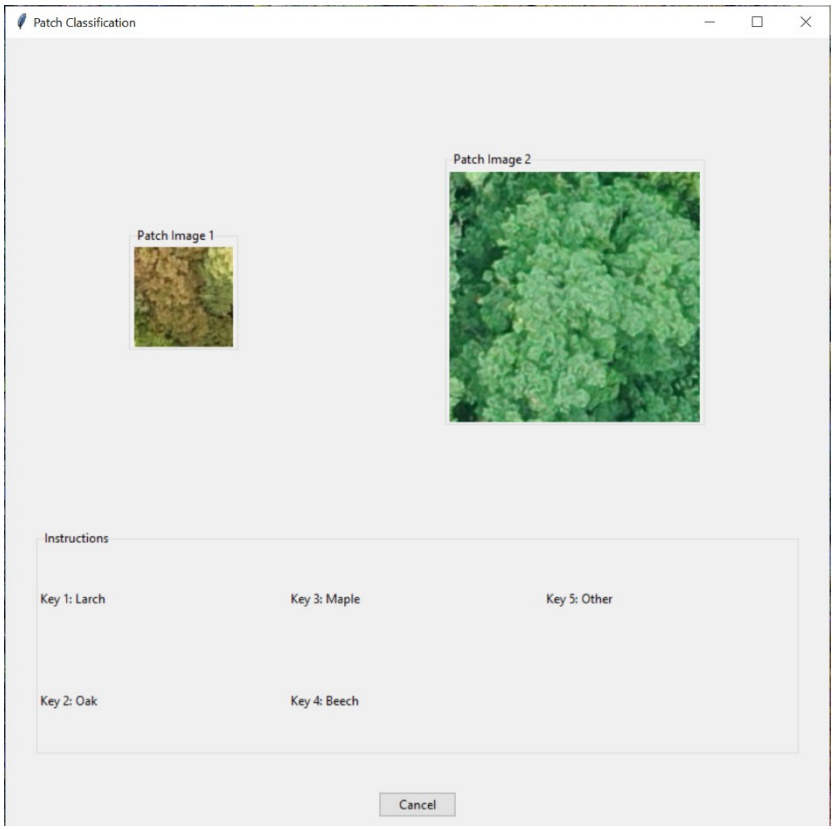


Figure 4.5: Tree classifier executable interface showing oak tree in autumn and summer and define button per species.

## 4.3 Results

### 4.3.1 Nitrogen content measurement

Foliar Nitrogen content was similar for the four tree species. The values were 2.01, 2.12, 1.93 and 1.94 wt.% respectively for larch, maple, beech and oak. Larch showed the highest nitrogen isotope $\delta^{15}N$ value (1.16‰) while maple present the lowest value (-4.37‰). Beech and oak nitrogen isotope $\delta^{15}N$ were similar.

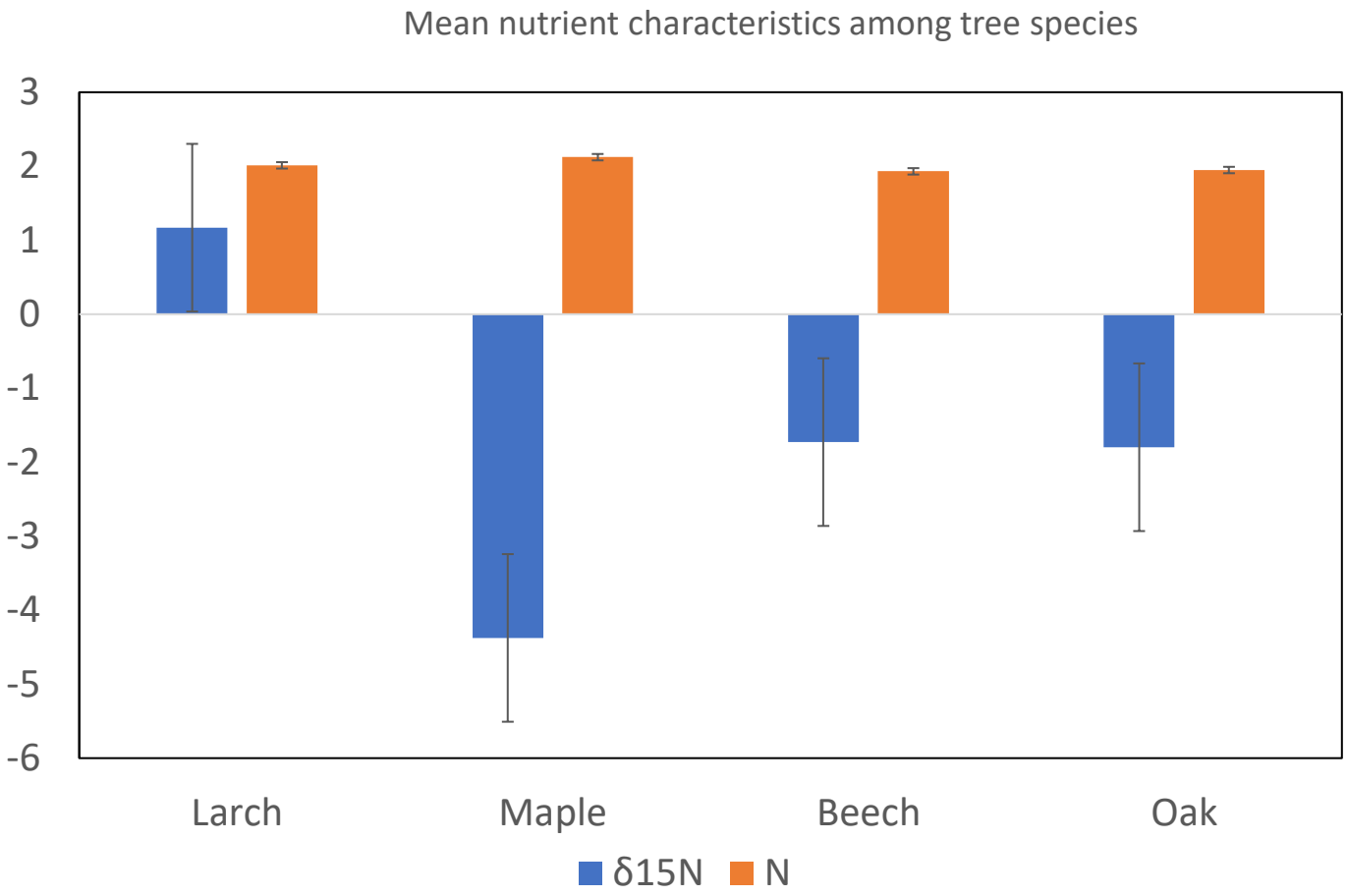


Figure 4.6: larch oak and beech nitrogen contain (orange) (wt.%)) and $\delta^{15}N$ (bleu) graph.

### 4.3.2 Pre-processed data

The identification was bases on two orthomosaic from summer and autumn (Figure 4.7)

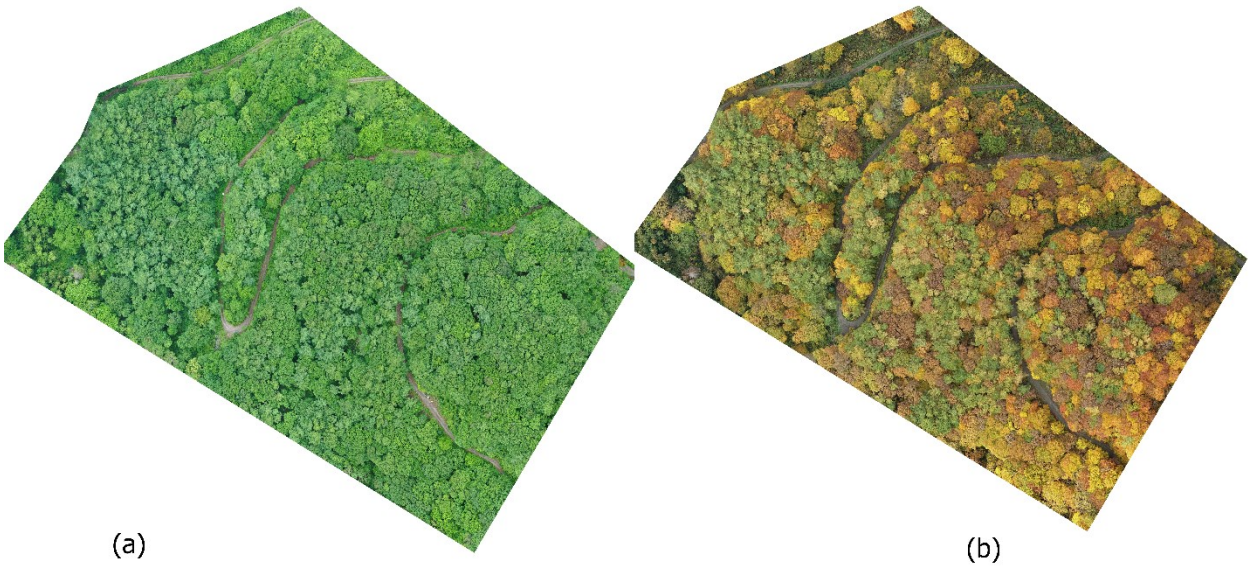


Figure 4.7 (a) autumn study site orthomosaic using Mavic2pro and (b) autumn orthomosaic using Phantom4RTK.

### 4.3.3 Tree species identification

In total 840 trees were annotated (Figure 4.8). Larche tree show the highest number of the annotated trees with 351 treetops while only 3 maple tops were marked (visible). Larch and beech annotated treetops were 351 and 141 respectively.

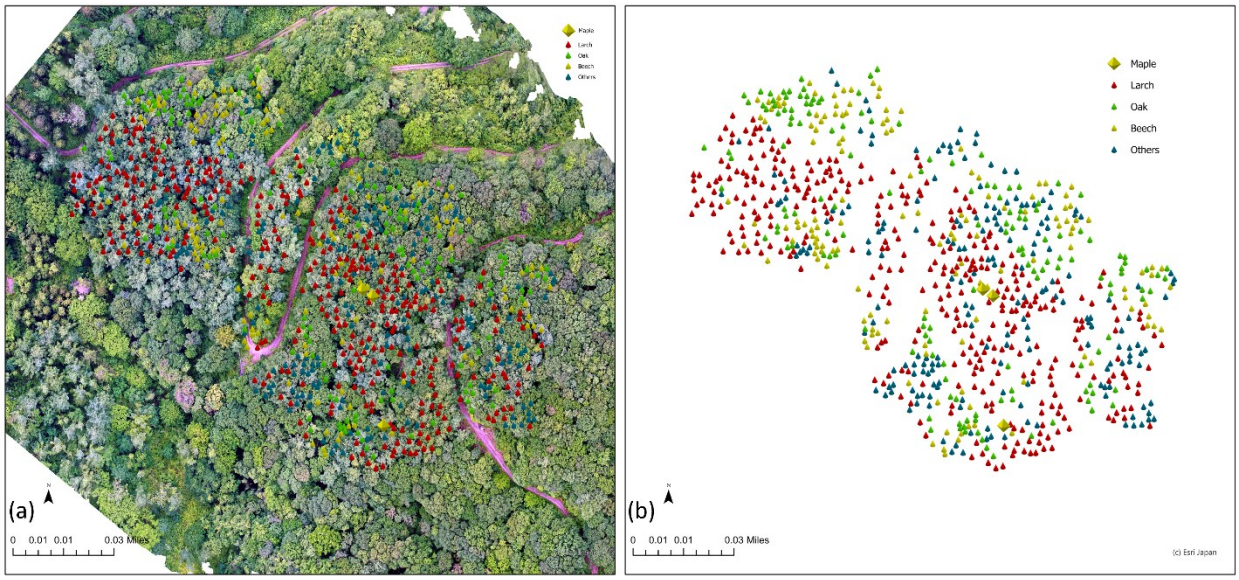


Figure 4.8:Treetops annotation on (a) summer orthomosaics and (b) treetops layer.

### 4.3.4 Nitrogen $\delta^{15}N$ value

Nitrogen isotope signal map (Figure 4.9 ) showed clearly the highest value (larch with 1.16‰) .

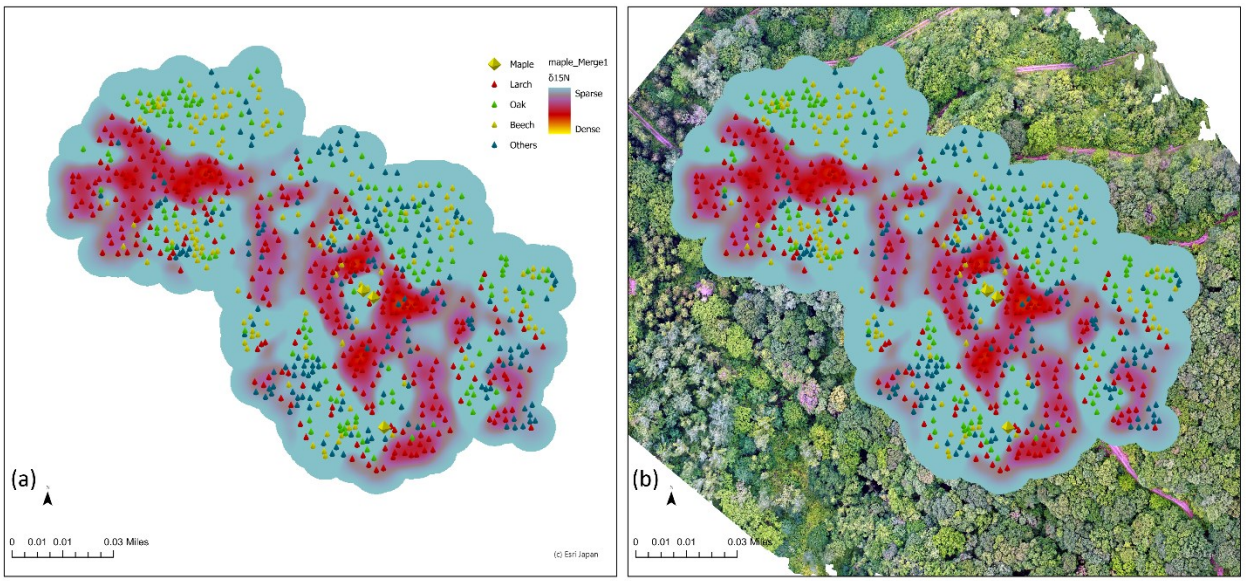


Figure 4.9: Treetops heatmap weight by nitrogen $\delta^{15}N$ value.

## 4.4 Discussion

In this chapter we make case that using very high resolution of UAV acquired orthomosaic in combination with field work measured data, we can provide accurate scaled up from tree to forest stand level. We took advantage of deciduous species seasonal change for four tree species identification. Changes in tree foliage colors help tree recognition in autumn which would be difficult in summer due to the low nuance of leaves green. This approach in not new though and has been used several times for tree identification (Park *et al.*, 2019; Yu *et al.*, 2021).

Patch based tree species identification isolate the tree and therefore in contrast to visualizing the whole orthomosaic, help to focus on only one object. In the current chapter two set of data, flying using terrain awareness function (summer) and at constant height (autumn) were used. Autumn generated patches show smaller size than summer patches and suggest that TAF orthomosaic was qualitatively better (Gonroudobou *et al.*, 2022).

The tree species in the study tend to grow clustered (Figure 4.8). The few numbers of maple trees can be explained by the fact that in this area there are small under the big tree canopy to be seen in the orthomosaic as they are covered by bigger trees

In this study we focused on four tree species Nitrogen content and isotope $\delta^{15}N$ value. Nitrogen content was not significantly different for all the species; a value map would have been not shown tree distribution or forest composition. Thus, only $\delta^{15}N$ value were used for scaled up map. Nitrogen isotope signal heatmap showed two principal tones (Figure 4.9) mainly from larch (highest value with 1.16) and oak and beech (very similar value). Even do maple isotope signal was clearly different (-4.37) the poor effective (3 treetops) did not make it visible on the map.

## 4.5 Conclusion

In this study we make use of larch, oak, maple and beech seasonal change and patches base python classifier assistance to annotate treetops. By combining field measurement and UAV acquired image orthomosaic we could scale up from tree to stand level Nitrogen isotope signal values.

Thus, we could accurately identify tree species and establish $\delta^{15}N$ signal distribution at forest stand scale.

## Bibliography

Aicardi, I. *et al.* (2016) 'Monitoring post-fire forest recovery using multi-temporal Digital Surface Models generated from different platforms.' EARSeL eProceedings. doi:10.12760/01-2016-1-01.

Battulwar, R. *et al.* (2020) 'A Practical Methodology for Generating High-Resolution 3D Models of Open-Pit Slopes Using UAVs: Flight Path Planning and Optimization', *Remote Sensing*, 12(14), p. 2283. doi:10.3390/rs12142283.

Bolelli, F. *et al.* (2020) 'Spaghetti Labeling: Directed Acyclic Graphs for Block-Based Connected Components Labeling', *IEEE Transactions on Image Processing*, 29, pp. 1999–2012. doi:10.1109/TIP.2019.2946979.

Bradski, G. (2000) 'The OpenCV Library.', *Dr. Dobb's Journal: Software Tools for the Professional Programmer*, 25(11). Available at: https://elibrary.ru/item.asp?id=4934581 (Accessed: 15 May 2022).

Cabezas, M. *et al.* (2020) 'Detection of Invasive Species in Wetlands: Practical DL with Heavily Imbalanced Data', *Remote Sensing*, 12(20), p. 3431. doi:10.3390/rs12203431.

Calders, K. *et al.* (2020) 'Terrestrial laser scanning in forest ecology: Expanding the horizon', *Remote Sensing of Environment*, 251, p. 112102. doi:10.1016/j.rse.2020.112102.

Čermák, J., Kučera, J. and Nadezhdina, N. (2004) 'Sap flow measurements with some thermodynamic methods, flow integration within trees and scaling up from sample trees to entire forest stands', *Trees*, 18(5), pp. 529–546. doi:10.1007/s00468-004-0339-6.

Chakraborty, K. *et al.* (2019) 'Forest biometric parameter extraction using unmanned aerial vehicle to aid in forest inventory data collection', *Current Science (00113891)*, 117(7), pp. 1194–1199. doi:10.18520/cs/v117/i7/1194-1199.

Cook, K.L. (2017) 'An evaluation of the effectiveness of low-cost UAVs and structure from motion for geomorphic change detection', *Geomorphology*, 278, pp. 195–208. doi:10.1016/j.geomorph.2016.11.009.

Davies, S.J. *et al.* (2021) 'ForestGEO: Understanding forest diversity and dynamics through a global observatory network', *Biological Conservation*, 253, p. 108907. doi:10.1016/j.biocon.2020.108907.

Diez, Y. *et al.* (2020) 'Comparison of Algorithms for Tree-top Detection in Drone Image Mosaics of Japanese Mixed Forests':, in *Proceedings of the 9th International Conference on Pattern Recognition Applications and Methods*. *9th International Conference on Pattern Recognition Applications and Methods*, Valletta, Malta: SCITEPRESS - Science and Technology Publications, pp. 75–87. doi:10.5220/0009165800750087.

Diez, Y. *et al.* (2021) 'Deep Learning in Forestry Using UAV-Acquired RGB Data: A Practical Review', *Remote Sensing*, 13(14), p. 2837. doi:10.3390/rs13142837.

FAO (2022) *Basic knowledge | SFM Toolbox | Food and Agriculture Organization of the United Nations*. Available at: https://www.fao.org/sustainable-forest-management/toolbox/modules/mountain-forests/basic-knowledge/en/ (Accessed: 30 April 2022).

Ferreira, M.P. *et al.* (2020) 'Individual tree detection and species classification of Amazonian palms using UAV images and deep learning', *Forest Ecology and Management*, 475, p. 118397. doi:10.1016/j.foreco.2020.118397.

Fleming, A.L., Wang, G. and McRoberts, R.E. (2015) 'Comparison of methods toward multi-scale forest carbon mapping and spatial uncertainty analysis: combining national forest inventory plot data and landsat TM images', *European Journal of Forest Research*, 134(1), pp. 125–137. doi:10.1007/s10342-014-0838-y.

Forestry Agency, Japan (2019) *3rd Country Report of Japan to the Montreal Process*. Available at: https://www.maff.go.jp/e/policies/forestry/attach/pdf/index-8.pdf.

Geng, J. *et al.* (2021) 'Evaluation of GOFP over four forest plots using RAMI and UAV measurements', *International Journal of Digital Earth*, 14(10), pp. 1433–1451. doi:10.1080/17538947.2021.1936226.

Getzin, S., Nuske, R.S. and Wiegand, K. (2014) 'Using Unmanned Aerial Vehicles (UAV) to Quantify Spatial Gap Patterns in Forests', *Remote Sensing*, 6(8), pp. 6988–7004. doi:10.3390/rs6086988.

Gonroudobou, O.B.H. *et al.* (2022) 'Treetop Detection in Mountainous Forests Using UAV Terrain Awareness Function', *Computation*, 10(6), p. 90. doi:10.3390/computation10060090.

Grêt-Regamey, A. and Weibel, B. (2020) 'Global assessment of mountain ecosystem services using earth observation data', *Ecosystem Services*, 46, p. 101213. doi:10.1016/j.ecoser.2020.101213.

Gupta, S.K. and Pandey, A.C. (2021) 'Spectral aspects for monitoring forest health in extreme season using multispectral imagery', *The Egyptian Journal of Remote Sensing and Space Science*, 24(3, Part 2), pp. 579–586. doi:10.1016/j.ejrs.2021.07.001.

Hartl-Meier, C. *et al.* (2014) 'Mountain forest growth response to climate change in the Northern Limestone Alps', *Trees*, 28(3), pp. 819–829. doi:10.1007/s00468-014-0994-1.

Hobbie, E.A. and Hobbie, J.E. (2008) 'Natural Abundance of 15N in Nitrogen-Limited Forests and Tundra Can Estimate Nitrogen Cycling Through Mycorrhizal Fungi: A Review', *Ecosystems*, 11(5), p. 815. doi:10.1007/s10021-008-9159-7.

Holtgrieve, G.W. *et al.* (2011) 'A Coherent Signature of Anthropogenic Nitrogen Deposition to Remote Watersheds of the Northern Hemisphere', *Science*, 334(6062), pp. 1545–1548. doi:10.1126/science.1212267.

Iglhaut, J. *et al.* (2019) 'Structure from Motion Photogrammetry in Forestry: a Review', *Current Forestry Reports*, 5. doi:10.1007/s40725-019-00094-3.

Jayathunga, S., Owari, T. and Tsuyuki, S. (2019) 'Digital Aerial Photogrammetry for Uneven-Aged Forest Management: Assessing the Potential to Reconstruct Canopy Structure and Estimate Living Biomass', *Remote Sensing*, 11(3), p. 338. doi:10.3390/rs11030338.

Kahmen, A. *et al.* (2006) 'Niche Complementarity for Nitrogen: An Explanation for the Biodiversity and Ecosystem Functioning Relationship?', *Ecology*, 87(5), pp. 1244–1255. doi:10.1890/0012-9658(2006)87[1244:NCFNAE]2.0.CO;2.

Kanno, M. *et al.* (2004) 'Geographical distribution of two haplotypes of chloroplast DNA in four oak species (Quercus) in Japan', *Journal of Plant Research*, 117(4), pp. 311–317. doi:10.1007/s10265-004-0160-8.

Kattenborn, T. *et al.* (2019) 'UAV data as alternative to field sampling to map woody invasive species based on combined Sentinel-1 and Sentinel-2 data', *Remote Sensing of Environment*, 227, pp. 61–73. doi:10.1016/j.rse.2019.03.025.

Kentsch, S. *et al.* (2020) 'Computer Vision and Deep Learning Techniques for the Analysis of Drone-Acquired Forest Images, a Transfer Learning Study', *Remote Sensing*, 12(8), p. 1287. doi:10.3390/rs12081287.

Khosravipour, A. *et al.* (2015) 'Effect of slope on treetop detection using a LiDAR Canopy Height Model', *ISPRS Journal of Photogrammetry and Remote Sensing*, 104, pp. 44–52. doi:10.1016/j.isprsjprs.2015.02.013.

Kikuchi, S. *et al.* (2009) 'Analysis of the disassortative mating pattern in a heterodichogamous plant, Acer mono Maxim. using microsatellite markers', *Plant Ecology*, 204(1), pp. 43–54. doi:10.1007/s11258-008-9564-1.

Kopačková-Strnadová, V. *et al.* (2021) 'Canopy Top, Height and Photosynthetic Pigment Estimation Using Parrot Sequoia Multispectral Imagery and the Unmanned Aerial Vehicle (UAV)', *Remote Sensing*, 13(4), p. 705. doi:10.3390/rs13040705.

Kozmus Trajkovski, K., Grigillo, D. and Petrovič, D. (2020) 'Optimization of UAV Flight Missions in Steep Terrain', *Remote Sensing*, 12(8), p. 1293. doi:10.3390/rs12081293.

Kulonen, A. *et al.* (2018) 'Enough space in a warmer world? Microhabitat diversity and small-scale distribution of alpine plants on mountain summits', *Diversity and Distributions*, 24(2), pp. 252–261. doi:10.1111/ddi.12673.

Lecointe, S. *et al.* (2006) 'Estimation of carbon stocks in a beech forest (Fougères Forest – W. France): extrapolation from the plots to the whole forest', *Annals of Forest Science*, 63(2), pp. 139–148. doi:10.1051/forest:2005106.

Leghari, S.J. *et al.* (2016) 'Role of nitrogen for plant growth and development: a review', *Advances in Environmental Biology*, 10(9), pp. 209–219.

Leidemer, T. *et al.* (2022) 'Classifying the Degree of Bark Beetle-Induced Damage on Fir (Abies mariesii) Forests, from UAV-Acquired RGB Images', *Computation*, 10(4), p. 63. doi:10.3390/computation10040063.

Li, J. *et al.* (2019) '3D Forest Mapping Using A Low-Cost UAV Laser Scanning System: Investigation and Comparison', *Remote Sensing*, 11(6), p. 717. doi:10.3390/rs11060717.

Lisein, J. *et al.* (2013) 'A Photogrammetric Workflow for the Creation of a Forest Canopy Height Model from Small Unmanned Aerial System Imagery', *Forests*, 4(4), pp. 922–944. doi:10.3390/f4040922.

Lopez Caceres, M.L. *et al.* (2018) 'Evaluation of the effect of the 2011 Tsunami on coastal forests by means of multiple isotopic analyses of tree-rings', *Isotopes in Environmental and Health Studies*, 54(5), pp. 494–507. doi:10.1080/10256016.2018.1495203.

Manconi, A. *et al.* (2019) 'Technical note: optimization of unmanned aerial vehicles flight planning in steep terrains', *International Journal of Remote Sensing*, 40(7), pp. 2483–2492. doi:10.1080/01431161.2019.1573334.

Messerli, B., Viviroli, D. and Weingartner, R. (2004) 'Mountains of the World: Vulnerable Water Towers for the 21st Century', *Ambio*, pp. 29–34.

Mohan, M. *et al.* (2017) 'Individual Tree Detection from Unmanned Aerial Vehicle (UAV) Derived Canopy Height Model in an Open Canopy Mixed Conifer Forest', *Forests*, 8(9), p. 340. doi:10.3390/f8090340.

Mohan, M. *et al.* (2021) 'Individual tree detection using UAV-lidar and UAV-SfM data: A tutorial for beginners', *Open Geosciences*, 13(1), pp. 1028–1039. doi:10.1515/geo-2020-0290.

Murata, K. *et al.* (2022) 'Effect of black locust trees on the nitrogen dynamics of black pine trees in Shonai coastal forest, Japan', *Plant and Soil* [Preprint]. doi:10.1007/s11104-022-05355-y.

Näsi, R. *et al.* (2015) 'Using UAV-Based Photogrammetry and Hyperspectral Imaging for Mapping Bark Beetle Damage at Tree-Level', *Remote Sensing*, 7(11), pp. 15467–15493. doi:10.3390/rs71115467.

Nguyen, H.T. *et al.* (2021) 'Individual Sick Fir Tree (Abies mariesii) Identification in Insect Infested Forests by Means of UAV Images and Deep Learning', *Remote Sensing*, 13(2), p. 260. doi:10.3390/rs13020260.

Nie, S. *et al.* (2019) 'Assessing the Impacts of Various Factors on Treetop Detection Using LiDAR-Derived Canopy Height Models', *IEEE Transactions on Geoscience and Remote Sensing*, 57(12), pp. 10099–10115. doi:10.1109/TGRS.2019.2931408.

Niethammer, U. *et al.* (2012) 'UAV-based remote sensing of the Super-Sauze landslide: Evaluation and results', *Engineering Geology*, 128, pp. 2–11. doi:10.1016/j.enggeo.2011.03.012.

Park, J.Y. *et al.* (2019) 'Quantifying Leaf Phenology of Individual Trees and Species in a Tropical Forest Using Unmanned Aerial Vehicle (UAV) Images', *Remote Sensing*, 11(13), p. 1534. doi:10.3390/rs11131534.

Pepe, M., Fregonese, L. and Scaioni, M. (2018) 'Planning airborne photogrammetry and remote-sensing missions with modern platforms and sensors', *European Journal of Remote Sensing*, 51(1), pp. 412–436. doi:10.1080/22797254.2018.1444945.

Puliti, S. *et al.* (2015) 'Inventory of Small Forest Areas Using an Unmanned Aerial System', *Remote Sensing*, 7(8), pp. 9632–9654. doi:10.3390/rs70809632.

Reed, S., Cleveland, C. and Townsend, A. (2011) 'Functional Ecology of Free-Living Nitrogen Fixation: A Contemporary Perspective', *Annual Review of Ecology, Evolution, and Systematics*, 42, pp. 489–512. doi:10.1146/annurev-ecolsys-102710-145034.

Rodríguez-Puerta, F. *et al.* (2022) 'UAV-Based LiDAR Scanning for Individual Tree Detection and Height Measurement in Young Forest Permanent Trials', *Remote Sensing*, 14(1), p. 170. doi:10.3390/rs14010170.

Rossini, M. *et al.* (2018) 'Rapid melting dynamics of an alpine glacier with repeated UAV photogrammetry', *Geomorphology*, 304, pp. 159–172. doi:10.1016/j.geomorph.2017.12.039.

Safonova, A. *et al.* (2019) 'Detection of Fir Trees (Abies sibirica) Damaged by the Bark Beetle in Unmanned Aerial Vehicle Images with Deep Learning', *Remote Sensing*, 11(6), p. 643. doi:10.3390/rs11060643.

Schulter, S., Leistner, C. and Bischof, H. (2015) 'Fast and Accurate Image Upscaling With Super-Resolution Forests', in. *Proceedings of the IEEE Conference on Computer Vision*

*and Pattern Recognition*, pp. 3791–3799. Available at: https://www.cv-foundation.org/openaccess/content_cvpr_2015/html/Schulter_Fast_and_Accurate_2015_CVPR_paper.html (Accessed: 1 May 2022).

Seidel, F. *et al.* (2019) 'Seasonal nitrogen partitioning in Japanese cedar (Cryptomeria japonica, D. Don) tissues', *Plant and Soil*, 442(1), pp. 511–529. doi:10.1007/s11104-019-04178-8.

Smith, T.M. and Urban, D.L. (1988) 'Scale and resolution of forest structural pattern', *Vegetatio*, 74(2), pp. 143–150. doi:10.1007/BF00044739.

Tateishi, M. *et al.* (2010) 'Differences in transpiration characteristics of Japanese beech trees, Fagus crenata, in Japan', *Tree Physiology*, 30(6), pp. 748–760. doi:10.1093/treephys/tpq023.

Thiel, C. and Schmullius, C. (no date) 'DERIVATION OF FOREST PARAMETERS FROM STEREOGRAPHIC UAV DATA – A COMPARISON WITH AIRBORNE LIDAR DATA', p. 8.

Tian, Q. *et al.* (2020) 'Variation of soil carbon accumulation across a topographic gradient in a humid subtropical mountain forest', *Biogeochemistry*, 149(3), pp. 337–354. doi:10.1007/s10533-020-00679-2.

Torresan, C. *et al.* (2017) 'Forestry applications of UAVs in Europe: a review', *International Journal of Remote Sensing*, 38(8–10), pp. 2427–2447. doi:10.1080/01431161.2016.1252477.

Vacik, H. and Lexer, M.J. (2014) ‘Past, current and future drivers for the development of decision support systems in forest management’, *Scandinavian Journal of Forest Research*, 29(sup1), pp. 2–19. doi:10.1080/02827581.2013.830768.

Valkaniotis, S., Papathanassiou, G. and Ganas, A. (2018) ‘Mapping an earthquake-induced landslide based on UAV imagery; case study of the 2015 Okeanos landslide, Lefkada, Greece’, *Engineering Geology*, 245, pp. 141–152. doi:10.1016/j.enggeo.2018.08.010.

Vitousek, P.M. *et al.* (2002) ‘Nitrogen and Nature’, *AMBIO: A Journal of the Human Environment*, 31(2), pp. 97–101. doi:10.1579/0044-7447-31.2.97.

*Welcome to Python.org* (no date) *Python.org*. Available at: https://www.python.org/ (Accessed: 15 May 2022).

Xiao, C., Qin, R. and Huang, X. (2020) ‘Treetop detection using convolutional neural networks trained through automatically generated pseudo labels’, *International Journal of Remote Sensing*, 41(8), pp. 3010–3030. doi:10.1080/01431161.2019.1698075.

Yang, W.-Q., Deng, R.-J. and Zhang, J. (2007) ‘[Forest litter decomposition and its responses to global climate change]’, *Ying yong sheng tai xue bao = The journal of applied ecology*, 18(12), pp. 2889–2895.

Yu, J.-W. *et al.* (2021) ‘Forest Vertical Structure Mapping Using Two-Seasonal Optic Images and LiDAR DSM Acquired from UAV Platform through Random Forest, XGBoost, and Support Vector Machine Approaches’, *Remote Sensing*, 13(21), p. 4282. doi:10.3390/rs13214282.

Zarco-Tejada, P.J. *et al.* (2001) 'Scaling-up and model inversion methods with narrowband optical indices for chlorophyll content estimation in closed forest canopies with hyperspectral data', *IEEE Transactions on Geoscience and Remote Sensing*, 39(7), pp. 1491–1507. doi:10.1109/36.934080.